UNIVERSITÀ DEGLI STUDI DI PADOVA

Dipartimento di Fisica e Astronomia "Galileo Galilei"

Tesi di Laurea in Fisica

Single File Diffusion with localized partial traps

Relatore:
Prof. Enzo Orlandini
Correlatore:
Dott. Fulvio Baldovin

Laureando: Martina Foglino
Matricola: 1080176

Anno Accademico 2014/2015

Contents

Abstract

Particle motion inside crowded or complex environments is a common phenomenon, from the microscopic to the macroscopic scales. It appears in many practical problems like human traffics, in fundamental biological mechanisms and in some industrial or chemical applications as well. Among these systems, the diffusion of hard-core particles in a channel so narrow that they cannot pass each other, know as Single File diffusion, has assumed a particular role since there is a large variety of systems in which such conditions are realized. Indeed, Single File Diffusion is responsible for the transport of ions in membrane channels, the diffusion in nano and micro-porous materials and has been observed in many artificial systems.

The task of this thesis is to investigate Single File systems of particles focusing on the effects on dynamical properties introduced by two different boundaries conditions: Absorbing Boundary conditions and Partially Reflecting ones. We develop both analytical and numerical results. The Single File system under examination will be addressed taking advantage of two important statistical analytical tools: the *Survival Probability density function*, i.e. the probability to find a particle, started from a certain initial position x_0, still between the considered boundaries at a certain time t, and the *Mean Emptying time*, i.e. the mean time needed for the channel system initially filled with a certain number of particles, in order to let all of them to exit from it, being absorbed by the boundaries. The theoretical analyses will be supported and compared to numerical results which have been obtained through molecular simulations performed using LAMMPS program. Such analysis will be performed for three specific cases:

- channel filled with one single Brownian particle;
- channel filled with many point-like Brownian particles under Single File condition;
- channel filled with many particles under Single File conditions, with introduction of volume exclusion effects.

Each of these cases will be considered under effects of two different boundaries conditions, absorbing and reflecting, pointing out the main difference in the dynamics.

Introduction

Since its discovery and development through the past century, Brownian motion has become a central paradigm in science [1]. Its characteristic energy and length scales make it widespread in soft matter Physics and Biology but it can also find many applications in other fields including ecology and economics, where diffusion-like equations are extensively used. Many systems, however, characterized by strong interactions, traps ,confinement, or self propulsion cannot be described by simple diffusion models as they show drastically different behaviors, generally named *Anomalous diffusion* [2] [3].

Indeed, deviations from free Brownian motion have been observed in many cases. A particular relevant example, which will be treated in this thesis, is the diffusion of particles in a restricted or crowded environments. From micro and nano porous materials or nanochannels to intracellular transport processes, particles are typically constricted by boundaries or by obstacles that considerably limit the space available for their motion. Example of confined diffusion can be found in biology, physiology, but also in chemistry and industrial applications. Diffusion of particles in Zeolites [7], catalytic reactions in porous material, separation techniques of size-dispersed particles on micro or nano scales [9] happen in extreme confinement conditions. Concerning the biological aspects, DNA translocations[4], protein transport in crowded fluids as cytoplasm and nucleoplasm and in general many intracellular transport process are subjected to strong spatial constraints.

A specific example of this kind is the diffusion of hard-core particles in Single File, i.e. in a channel so narrow that they can not pass each other. Single File Diffusion in fact, has a relevant importance in chemistry, physics and biology as it is responsible for the transport of ions in membrane channels and has been observed in a variety of artificial systems [6]. From the theoretical point of view, Single File Diffusion of particles is an exactly solvable model and provides a paradigmatic example of anomalous diffusion in crowded equilibrium system. The key feature of this kind of system is the preservation of the initial ordering, which force particles to hinder each other. The displacement of any particle requires the movement of some of the others in the same direction: from this extreme confinement strong correlations and subdiffusive behavior arise, where the Mean Squared Displacement $< x^2(t) >$ scales with $\sqrt{t}$ rather then t.

Thesis Outline: Aim of this thesis is to investigate the properties of diffusive particles under Single File conditions, focusing on the difference caused by imposing absorbing boundaries conditions or partially reflecting ones. We provide the exact solutions for the emptying process, i.e. the progressive decrease of particle inside the channel system due to the absorbing or partially reflecting boundaries, and we compare theoretical results with numerical simulations performed using the program LAMMPS.

In Chapter 1 we will give an overview of the most relevant issues related to the diffusion in confined or crowded environment, with particular attention to anomalous diffusion, supported by numerical simulations. In Chapter 2 we deal with the properties of Single File system of diffusing particles in the presence of two absorbing boundaries, with the comparison of analytical calculations and numerical simulations. We will look for the Survival Probability Density Function, i.e. the probability to find a particle between the absorbing boundaries at a time t. In particular, we will start with a single particle, verifying the analytical form of the Survival probability evaluated, and then we will consider the channel system composed by 10 non interacting particles, developing the same study. In the last section of Chapter 2 we will discuss the effects due to volume exclusion, presenting numerical results for the Survival Probability function. In Chapter 3 we will study the channel system previously considered, this time subjected to Partially Reflecting Boundaries conditions. We will focus on the analytical calculation for the Survival Probability function both for the case of single or many Brownian particles, presenting numerical results obtained trough simulations. Finally we will draw our conclusions.

Chapter 1

Diffusion under confinement

Particles diffusion under confinement plays an interesting role in Physics. Indeed, in many systems particles are confined in narrow or crowded environment like in the case of diffusion in Zeolites or Ion transport through nanopores. In this chapter we will present the basic tools needed for the description of Diffusion processes, starting from the central concept of Brownian motion and its description through Langevin and Fokker-Planck equations. All the described theoretical aspects will be then validated through numerical simulations performed using LAMMPS dynamical simulator, in particular the Einstein relation which links the diffusion coefficient with the system temperature will be verified. The role of anomalous diffusion will be emphasized considering its physical relevance in many physical problems. Numerical analysis will be extended to the case of anomalous diffusion showing the evidence of such peculiar motion in a simple system of crowded particles.

1.1 Tools about simple Diffusion

In order to give a proper theoretical description of the dynamics of Single File diffusion, it is necessary firstly to handle the basic principles of diffusion. As it is well known, a body immersed in a fluid experiences the action of the fluid elements in the surroundings, resulting in a random trajectory usually called Brownian or diffusive motion [1]. Described in terms of probability theory, at a given time t, the particle position is a random variable X. In order to characterized it, we introduce the probability density function $p_X(x)$

$$p_X(x) = Prob(x < X < x + dx) \tag{1.1}$$

representing the probability of finding a particle between the positions x and $x + dx$. A collection of such random variables, parametrized by time, is called *stochastic process*: in virtue of the Central Limit theorem [8], Brownian motion is one of the most important example. As different realizations of the evolution produce a completely different pattern for the observed physical quantities, such a motion is better analyzed in terms of statistical quantities like the first moment of the random variable:

$$\langle X \rangle = \int_{-\infty}^{\infty} x p_X(x) dx. \tag{1.2}$$

Since the mean value of the position $\langle X \rangle$ for a Brownian motion is zero because of the particle random trajectory, we have to consider another quantity which can define the evolution of motion. A simple way to analyze the dynamics of diffusion is taking into account the time evolution of the Mean Squared Displacement $\langle (X(t) - X_0)^2 \rangle$ where $X(t)$ is a stochastic process at time t, X_0 is the initial particles position and the average is made over many independent realizations. Indeed, such quantity is a common way to measure the amount of space explored by the system under examination. Considering a Brownian motion with trajectory $X(t)$, the Mean Squared Displacements has the following form [8]

$$\langle (X(t) - X_0)^2 \rangle = 2dDt \tag{1.3}$$

where d represents the spatial system dimension and D is called *Diffusion Coefficient* and represents the explored area per time unit. From now on, in this thesis we will only focus on the one dimensional case, thus the coefficient d presented above will be set to the value of 1.

Our numerical simulations rely on the Langevin model introduced in 1908 [19]. Langevin equation reads

$$m\dot{v} = F_e + F_t, \tag{1.4}$$

where F_e is a general external force, and F_t is the sum of the forces that each molecule of the fluid exerts on the mesoscopic particle. The last term represents two contributions:

- the deterministic damping term $-\alpha\vec{v}$;
- a fluctuating term $f(t)$ which represents the contributions of the continuous collisions of the fluid molecules with the mesoscopic particle, considering the latter as at rest.

Because of the stochastic nature of $f(t)$, we have to define its probability distribution and moments. The most simple choice is to consider a Gaussian noise defined by

- $\langle f(t) \rangle = 0$;
- $\langle f(t) f(t') \rangle = \delta(t - t')$.

The relevance of including an external force relies on the many physical applications it sees: in biology for example it is not uncommon to observe some external drag force which strongly affects the particles motion. For simplicity let's firstly neglect the external force, thus the Langevin equation becomes a stochastic system of differential equations:

$$m\frac{dv}{dt} = -\alpha v + f(t). \tag{1.5}$$

Defining the quantity $\gamma = \frac{\alpha}{m}$ we observe that on timescales τ such that $\gamma\tau >> 1$ (Over-damped limit), we obtain [19]:

$$v = \frac{dx}{dt} = \frac{1}{\gamma m} f(t). \tag{1.6}$$

From standard methods [19] it is possible to obtain an equivalent description of fluctuations in a Fokker-Planck formalism which provides a deterministic differential equation for the probability distribution function $p_1(x,t|x_0,1,L)$ of finding one particle in position x at time t within a channel system of length L, given that the initial coordinate at time zero is x_0. For Brownian motion in the overdamped limit such equations reads:

$$\frac{\partial p_1(x,t|x_0,1,L)}{\partial t} = D\frac{\partial^2 p_1(x,t|x_0,1,L)}{\partial^2 x} \ , \tag{1.7}$$

where the constant D is the Diffusion Constant which has been previously introduced in equation (1.3). Equation (1.7) will plays a fundamental role in this thesis, as we will address its solution by providing the probability distribution functions according to different boundaries conditions. In the following sections we will also present a numerical study in order to verify the Einstein relation:

$$D = \frac{K_b T}{\gamma m} = \frac{K_b T}{\alpha} \ , \tag{1.8}$$

where in the case under exam $\alpha = 6\pi r\eta$, with η the fluid viscosity and r is the particle radius. The equation (1.8) will be verified performing numerical simulations using LAMMPS program, as it will be clear from the next section.

1.2 Anomalous Diffusion

As anticipated, another important case which will be numerically treated in this thesis is the Anomalous diffusion. The interest in such case relies on the real situations in which such behavior can be detected. Just to give some examples we can consider confined nanofilms [21] [22], Single File diffusion, transport in porous media [23], fractal structures with holes over all length scales [24], charge-carrier transport in anomalous semiconductors [25]. One of the most common example of this kind of systems is a crowded fluid, a natural phenomenon in living cells with considerable impact on intracellular chemical reactions.

Consider, for example the presence of walls or obstacles in the system, then the amount space explored by the particles dynamics is considerably reduced and the Mean Squared Displacement time evolution becomes:

$$\langle x(t)^2 \rangle \propto t^{\beta} \ , \tag{1.9}$$

where $\beta < 1$ in this case and we have set the initial position X_0 to zero. On the other hand, examples of systems where particles motion is enhanced rather than decreased also exist so that a power law behavior like the previous one is observed but with $\beta > 1$. The first case is known as *Subdiffusion* while the second as *Superdiffusion*.

In the last years there have been many attempts to model anomalous diffusion through extension of the Fokker-Planck equation by incorporating fractional derivatives, non linear terms [26] or spacial and time dependence in the diffusion coefficient [27]. In this thesis it will be studied the dynamics of a system composed by a narrow channel filled with point-like interacting particles. As it will be clear later from numerical results, there are two different behaviors depending on the boundary conditions chosen. With reflecting boundary

conditions, i.e. a close channel, the dynamics is dominated by a subdiffusive behavior caused by the crowded environment. With periodic boundary conditions at the border of the channel axes, one can distinguish an initial dynamics dominated by subdiffusive behavior followed by a longer and stable diffusion for the rest of time evolution. Finally, considering absorbing boundary conditions, we can expect to see an initial subdiffusive motion in the case of high density of particles or a diffusive motion in the case of low density.

1.3 Numerical Analysis

The previous phenomenology can be studied through numerical simulations describing the diffusive behavior of particles in one dimension. Such a system can be easily represented by a channel of fixed length filled with a certain number of point-like particles. Before introducing the numerical tools used to build the channel system and to perform the simulations, a brief digression is needed to define the units of measure used. Using LAMMPS simulator we firstly have to define the units we require [20]. Through the proper command, we set the style of units used for a simulation, thus determining the units of all quantities specified in the input script and data file as well as quantities output. The choice we made in the simulations of this thesis is the style lj (Lennard Jones). This style is based on the Lennard Jones potential

$$V = 4\epsilon\Big[\Big(\frac{\sigma}{r}\Big)^{12} - \Big(\frac{\sigma}{r}\Big)^{6}\Big] \text{if } r < r_c \tag{1.10}$$

where ϵ is the depth of potential well, σ is the finite distance at which the interparticle potential is zero, r is the distance between the interacting particles and r_c is the cutoff, with $r_c > \sigma$. For the style lj, all quantities are unitless. Without loss of generality, LAMMPS sets the fundamental quantities mass, sigma, epsilon, and the Boltzmann constant K_b to 1. The masses, distances, energies one can specify are multiples of these fundamental values thus generating reduced, or unitless quantities, referred to with an asterisk by assigning specific values to the above constants. It is still possible to convert such quantities to dimensional one, using the following relations:

- distance $x^* = \frac{x}{\sigma}$;
- time $t^* = t\sqrt{\frac{\epsilon\sigma^2}{m}}$;
- energy $E^* = \frac{E}{\epsilon}$;
- temperature $T^* = \frac{TK_b}{\epsilon}$.

Keeping in mind such a possibility, in what follows all the physical quantities will be reported dimensionless.

The first system which has been studied is composed by 10 point particles of identical types and unitary masses in a box, with periodic boundary conditions chosen to be at positions -50 and 50 (lj units). Firstly, volume exclusions effects have been neglected. All particles are, at the beginning of the simulations, in random initial position. The LAMMPS code evaluates at each step all the atoms positions (x,y,z) and velocities. In order to avoid starting with a too sharp potential which could be computationally demanding, we

recreated the one dimensional system through a step by step strategy. First we considered a three dimensional box and then, during the first run of the program we progressively confine the system particles forcing them into a fixed coordinate along the z-axis, thus generating a sort of two dimensional system. From such a plane, we introduce a cylindrical potential in order to confine all particles inside a channel of radius 1 and length 100.

Having build the "channel system", characterized by periodic conditions over the x axis direction, our first concern is to verify the diffusion law (1.3) and in particular the Einstein's relation (1.8)

1.3.1 Simple one-dimensional diffusion

In order to verify (1.8) and (1.3) we perform 1000 runs of LAMMPS program. We collect the results averaging the Mean Squared Displacement over the 1000 runs, and then, since the particles are free, we also average over the 10 particles, obtaining just one function reported in Figure 1.1:

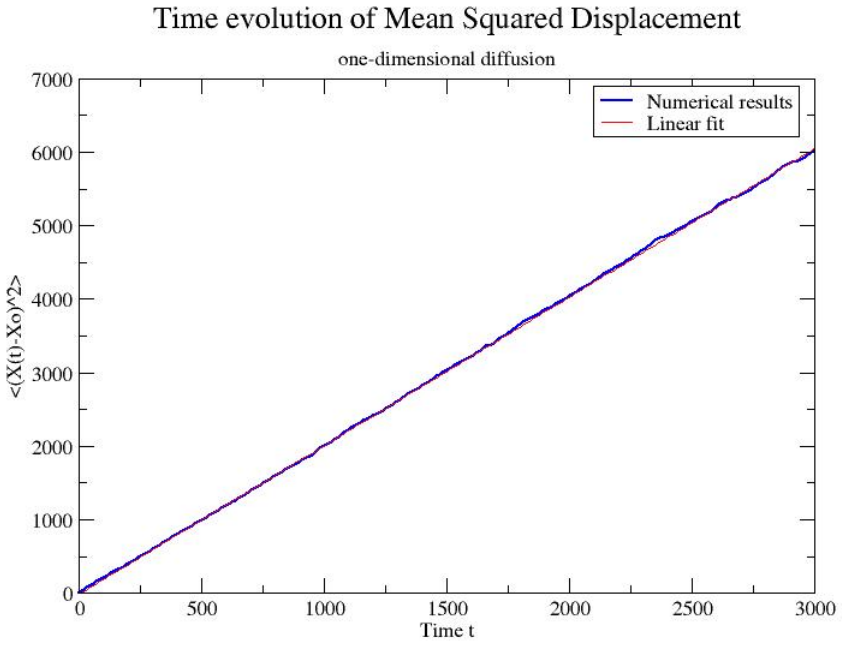

Figure 1.1: Plot of the MSD of 10 point-like interacting particles in 1D system vs time. The single line (obtained averaging over 1000 runs of 3000000 steps (timestep = 0.001) and then averaging over the 10 point non-interacting particles) represents the MSD trend during time evolution of the global system.

Performing a linear fit we obtained the following values:

$$\begin{aligned} a &= 2.02 \\ b &= -18.2 \end{aligned} \tag{1.11}$$

From the previous values we can derive, from the Diffusion equation (1.3), the coefficient $D = \frac{a}{2} = 1.011 \pm 0.001$. Because of the simulation setting we have $K_b = 1$, $\gamma = 1$, $m = 1$ and the temperature, averaged over the 1000 runs is $T = 1.1$. With these parameters, the Diffusion Coefficient derived from (1.8) is $D = T = 1.1$. As another way to evaluate the Diffusion Coefficient, we plot the Mean Squared Displacements divided over time in order to find an approximately constant function which should be proportional to the Diffusion Coefficient D. The result is in Figure 1.2

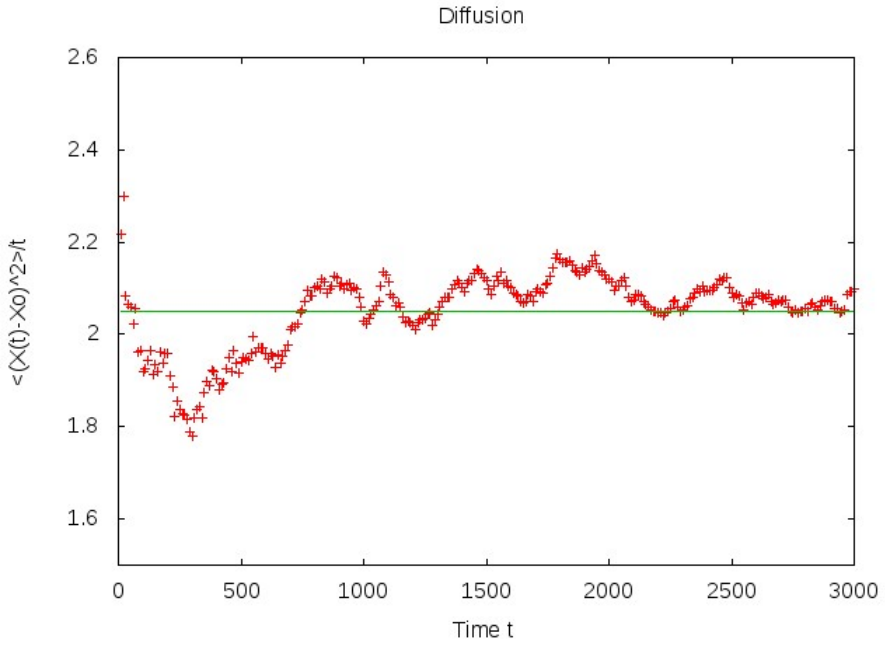

Figure 1.2: Plot of the mean squared displacements of 10 point-like particles in 1D system divided for each timestep of a single atom. The approximately constant trend obtained averaging over 1000 runs, is proportional to the Diffusion Coefficient D

The fit with the constant function $f(x) = a$ gives$a = 2.05$. From this value we can derive the Diffusion Coefficient as $D = \frac{a}{2} = 1.03$. A rough estimate of the error for to the Diffusion coefficient can be found simply considering two sets of data and comparing the results obtained using each of them. We followed the same method as previously described for two sets of 500 runs each, performing two linear fits. The value obtained are the following:

- fit with the first set of 500 simulations: $a_1 = 2.076 \pm 0.001$
- fit with the second set of 500 simulations: $a_2 = 2.011 \pm 0.002$

The difference between the two value obtain is $a_1 - a_2 = 0.065$. If we consider this value as the error related to equation (1.11), we obtain: $a = 2.02 \pm 0.07$, thus $D = a/2 = 1.01 \pm 0.04$. Considering that the expected value is $D = 1.1$, the estimate obtained with this last error shows an acceptable compatibility with the expected one.

1.3.2 One-dimensional anomalous diffusion

We now try to simulate the particles motion generated in a crowded environment adapting the channel system previously used for our task. The channel is now still filled with 10

particles, but, in order to recreate the crowd we are looking for, we introduced a Lennard Jones potential among particles, modeling a volume excluded effects. In this way, particles motion is affected by the neighbors presence, thus generating obstacles which modify their trajectories.

Numerically, the system under exam is described using two types of boundary conditions, the periodic and the reflecting ones, underlining the difference between the two cases. Let's first focus on the periodic boundary conditions at the border of the channel. Numerical integration takes into account the space explored by the particles adding the channel length value L every time they periodically exit and enter from the other side. In this way the system we consider is actually an infinite channel. We expected our 1000 simulations to show the combination of two regimes: first a short period of subdiffusion, caused by the crowded environment, followed by a longer period of diffusion because the periodic boundary conditions let the particles to diffuse normally, being dilute along the channel.

The following Figures graphically represent the motion trend we just explained. First, we consider a single point-particle initially positioned at the center of the channel, which is globally filled with other 9 particles interacting among themselves through a Lennard Jones potential. As we can see from Figure 1.3, the mean squared displacement divided over time of the considered central particle shows a trend which can be seen as the combination of two part: first it decreases rapidly and then it stabilizes to an approximately constant value. These two contributions can be interpreted as defining two different motion behaviors: the rapid decrease is linked to a subdiffusive behavior, while the constant trend is referred to a diffusive one. Calculating the average values over the 1000 simulations, we can recognize the two trends discussed above from the following Figure 1.3:

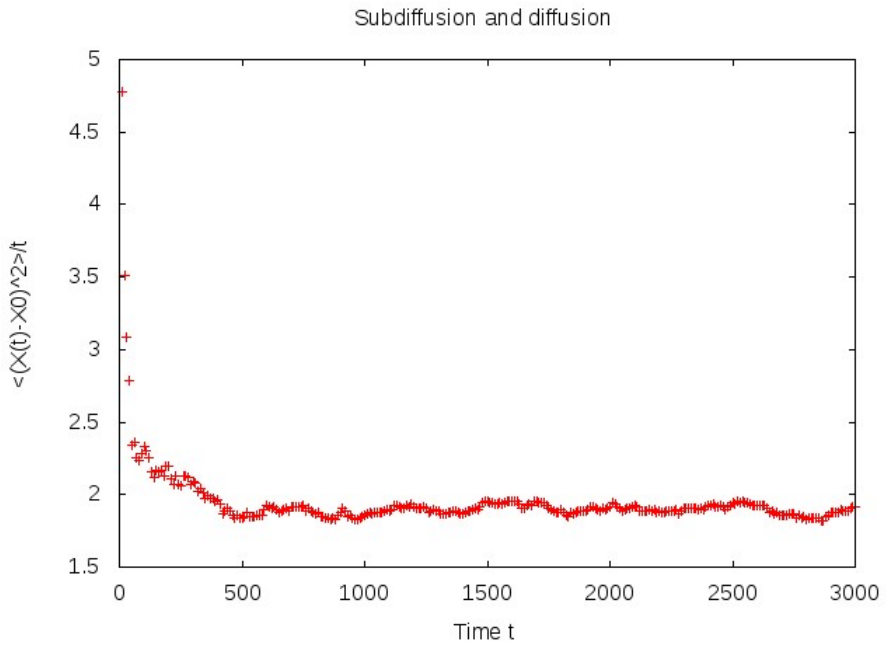

Figure 1.3: Plot of the mean squared displacement divided for time of a single point-particle in the middle of the channel, among 10 interacting particles in 1D system over time. The single line is obtained averaging over 1000 runs.

As we previously anticipated, we also simulated the channel system characterized with

reflecting boundary conditions, modeling a close channel, in order to observe mutations in particles diffusive motion. The channel itself remains unchanged, it is filled with 10 interacting particles this time subjected to reflecting boundary conditions at the borders. Without the possibility for each particle to exit from the system, the environment becomes more crowded than the one characterized by periodic boundary conditions. Interacting particles keep colliding with themselves thus generating a system filled with many obstacles which actually affect the diffusion motion. All of these conditions cause the particles to perform a subdiffusive motion from the beginning of time evolution, and forbid the adjustment of motion to a diffusive one. In order to show the difference between the two cases we plot the same Figure consisting of the mean squared displacements divided over time of the central particle. From Figure 1.4 we can recognize just one single trend, in fact the line representing the mean squared displacements over time does not approach to a constant value as it did for the periodic boundary conditions. Such line keeps decreasing showing that for these kind of boundary conditions the particles motion is always subdiffusive, because the crowd environment does not allow particles to freely diffuse. The figure below is obtained performing 1000 simulations.

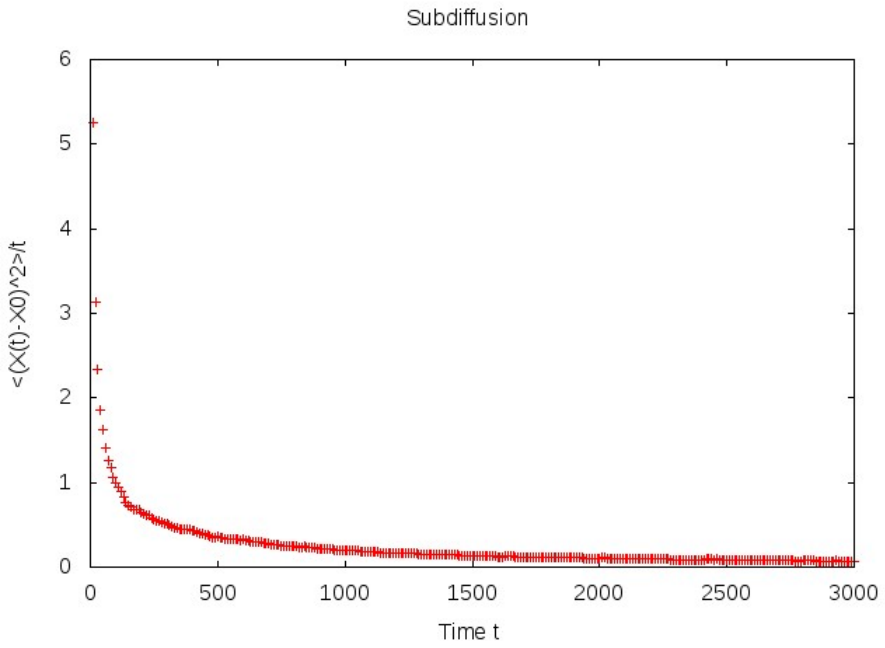

Figure 1.4: Plot of the mean squared displacement divided for time of the particle approximately in the middle of the channel, among 10 interacting particles with volume excluded effects in 1D system over time. The single line is obtained averaging over 1000 runs.

Chapter 2

Emptying processes in Single File diffusion systems

In this Chapter we will present an overview of the theoretical literature on Single File diffusion, i.e. diffusion from a channel so narrow that particles order is strictly preserved. In this part of the thesis our aim is to develop an analytical study of the Emptying process of the system, i.e. the progressive decrease of the number of particles in a region of interest due to absorbing boundaries conditions, either in presence or absence of an external force. The relevance of this second case relies on the many physical applications it sees: in biology for example it is not uncommon to observe some external drag force which strongly affects the particles motion. Such external force can be represented by the gravitational field itself. We first consider the simplest case of a single a simple Brownian particle in presence of two absorbing boundaries and of a constant external force F_e. Furthermore, we will introduce the concept of Survival Probability density function and the Mean First Passage Time as valid instruments to study the emptying process. By means of the Fokker Planck equation formalism introduced in the previous chapter, we will derive analytical solutions for the probability distribution function in a one dimensional channel, as well as for its Survival Probability. The same analysis will be then performed for the system composed of many point-like particles, where volume excluded effects have been neglected. The exact solutions to these problems will be then validated by comparison with numerical simulations. The last section of this Chapter presents a theoretical discussion and numerical simulation on the effect that excluded volume interactions between particles may have on the Emptying process in single file systems.

2.1 Theoretical Description of Single File Diffusion

Single File constraint can be seen as an ideal representation of en extreme channel-like confinement where particles maintain spatial order during their motion [10]. As a result of this strongly correlated dynamics, particles perform a subdiffusive motion which lasts for a very long time if their number is large enough [11]. In order to find an analytical description of Single File Diffusion we made use of an important theoretical tool: the Reflection Principle method [13]. It consists of a mapping of the interacting system on a non-interacting one considering Single File diffusion as a free particles diffusion in which at each collision particles simply exchange their labels. Thus, each possible collision between neighboring particles is taken into account as a switch of the indexes of the two non interacting particles thus transferring the boundary condition problem for the Green's function of the entire interacting system to the Green's function of the freely diffusing particles. This method can be schematically expressed through Figure 2.1 :

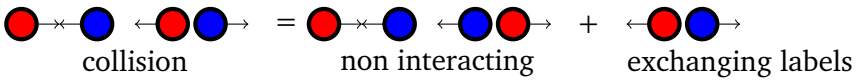

Figure 2.1: Schematic motion of Brownian particles with interacting collisions. In an equivalent non-interacting picture, on the right side, we allow particles to pass through each other. The path of a pair of particles experiencing an hard-core collisions event can be represented by two noninteracting particles passing through each other and having their labels switched.

We have to remark that this method, although quite simple to use, does have some limitations. Indeed, in order to apply the Reflection Principle Method the particles must be identical and the collisions have to be elastic, otherwise it would not be possible to exchange positions and velocities. In such one-dimensional channel system spatial order is strictly preserved because of the impossibility of crossing during all dynamical evolution. This imply that only a section A of the entire configurations space is accessible. Such section is defined by the planes $x_i = x_j \forall i, j$. The " non-crossing" property can be therefore expressed as the condition that the flux trough these planes vanishes, i.e. they act as reflecting boundaries. As in the case of usual reflecting boundaries, this conditions can be satisfied using the *reflection principle* [13]: if a solution is reflected at the interesting point and added to the original solution, the derivative of the sum normal to this plane vanishes. In this contest all particles act as reflecting planes so it is necessary to consider all possible reflections, which imply a simple change of coordinates. The combinations of all possible reflections are given by the permutations of the particles coordinates, so that the probability density function $p_N(\mathbf{x}, t|\mathbf{x}^0, N, L)$ of finding the Single File array of particles in positions $\mathbf{x} = (x_1, x_2, ..., x_N)$ at time t within a channel centered in $x = 0$ of width L, given that the initial coordinates at time zero are $\mathbf{x}^0 = (x_1^0, x_2^0, ..., x_N^0)$ with $-L/2 \leqslant x_1^0 < x_2^0 < ... < x_N^0 \leqslant L/2$ is provided by the following expression:

$$p_N(\mathbf{x}, t|\mathbf{x}^0, N, L) = \begin{cases} \sum_{x \in \Pi_N} \prod_{k=1}^{N} p_1(\mathbf{x}_{\pi(k)}, t|\mathbf{x}^0, 1, L) & \mathbf{x} \in \mathrm{A} \\ 0 & \mathbf{x} \notin \mathrm{A} \end{cases} \tag{2.1}$$

where Π_N is the set of permutations of N objects and *A* represents the set of allowed configurations defined by

$$\mathrm{A} = (-L/2 \leqslant x_1 < x_2 < ... < x_N \leqslant L/2), \tag{2.2}$$

and the function $p_1(\mathbf{x}_{\pi(k)}, t|\mathbf{x}^0, 1, L)$ is the Green's function for the free single particle problem with absorbing boundary conditions at $x = \pm L/2$.

2.2 Emptying process

As explained in Chapter 1, the probabilistic approach used to treat this process relies on the concept of the conditioned probability distribution function $p_1(\mathbf{x}, t|\mathbf{x}^0, N, L)$. Such function can be obtained by solving equation (1.7), which is valid in the case of Brownian motion in the Overdamped limit. Through Fokker-Planck equation, it is possible to vary the boundary conditions, which depend on the problem under study. As we previously anticipated, we have extensively used absorbing boundary conditions in one dimension, i.e. particles are forever expelled from the system once they reach the boundary. In this context a meaningful quantity is the *Survival Probability density function* $S(t|\mathbf{x}^0, N, L)$, i.e. the probability that a single particle, started at position $\mathbf{x}(0) = \mathbf{x}_0$ inside the boundaries, has not been expelled up to time t. If we call by t^* the time of the exit event, the Survival Probability can be seen as

$$S(t|\mathbf{x}^0, N, L) = Prob(t^* > t). \tag{2.3}$$

In terms of probability distribution function this can be written as

$$S(t|\mathbf{x}^0, N, L) = \int_{b_1}^{b_2} p_1(\mathbf{x}, t|\mathbf{x}^0, N, L)dx \ , \tag{2.4}$$

where we have assumed two absorbing boundaries placed respectively at $x = b_1$ and $x = b_2$, $p_1(\mathbf{x}, t|\mathbf{x}^0, N, L)$ is the probability density function for the single particle and $L = |b_2 - b_1|$. Considering that our task is to study the emptying process, another fundamental quantity which will be of frequent use is the *Mean First Passage Time* $T(\mathbf{x}^0, N, L)$. Such quantity represents, as the name suggests, the mean time at which particles reach the absorbing boundary for the first time, thus exiting from the channel. The Mean First Passage Time can be defined as follows:

$$T(\mathbf{x}^0, N, L) := \int_0^\infty S(t|\mathbf{x}^0, N, L)dt. \tag{2.5}$$

Making use of the Reflection Principle method, we will now provide a detailed study of the case of a narrow channel of length L with two absorbing boundaries at $x = -L/2$ and $x = L/2$. We will study the emptying process of a system composed by point-like particles under Single File constraint. Even if equation (2.1) is exact, it is still difficult to handle both analytically and numerically because of the restriction of the allowed configurations. However, since our work is limited to the study of the emptying process, we are only interested in the Survival Probability of all the N particles which is

$$S_N(t|\mathbf{x}^0, N, L) = \int_A p_N(\mathbf{x}, t|\mathbf{x}^0, N, L)dx, \tag{2.6}$$

where *A* is the set of allowed configurations defined in the previous Section. In this case,

the permutations in equation (2.1) allow to remove the order constraint and one obtains:

$$\begin{aligned} S_N(t|\mathbf{x}^0,N,L) &= \int_A p_N(\mathbf{x},t|\mathbf{x}^0,N,L)dx = \\ &= \int_A \sum_{x\in\Pi_N}\prod_{k=1}^{N} p_1(\mathbf{x}_{\pi(k)},t|\mathbf{x}^0,1,L) = \\ &= \prod_{k=1}^{N}\int_A p_1(\mathbf{x}_{\pi(k)},t|\mathbf{x}^0,1,L) = \\ &= \prod_{k=1}^{N} S_1(t|\mathbf{x}_k^0,1,L), \end{aligned} \tag{2.7}$$

where $S_1(t|\mathbf{x}^0,1,L)$ is the survival probability of a single free particle placed initially in position x_k^0 and absorbed in $x=\pm L/2$. For the study of the emptying process of a Single File system of identical point-like particles, equation (2.7) can be used obtaining a fundamental simplification. If we indicate by $S_n(t|\mathbf{x}^0,N,L)$ the probability of having at least $0\leqslant n\leqslant N$ particles within the channel of length L, we have:

$$S_n(t|\mathbf{x}^0,N,L)=\sum_{k=n}^{N} p_k(t|\mathbf{x}^0,N,L). \tag{2.8}$$

Consequently, the channel emptying probability will be $1-S_1(t|\mathbf{x}^0,N,L)$. In the last equation $p_n(t|\mathbf{x}^0,N,L)$ is the probability of having n particles within the channel at time t, given that at time zero the N particles were located at $\mathbf{x}^0$. An equivalent way to define $p_n(t|\mathbf{x}^0,N,L)$ is to consider that n particles have first passage time at boundaries larger than t, while the other $N-n$ ones have it smaller than t. Thus, $p_n(t|\mathbf{x}^0,N,L)$ can be defined as

$$p_n(t|\mathbf{x}^0,N,L)=Prob(t_1^*,...,t_n^*>t,t_{n+1}^*,...,t_N^*<t|\mathbf{x}^0,N,L). \tag{2.9}$$

By taking advantage of equation (2.1) and since each particle is independent from each other, from (2.3) we obtain

$$p_n(t|x_0,N,L)=\frac{1}{n!(N-n)!}\sum_{\pi\in\Pi_N}\int_t^\infty dt_1...\int_t^\infty dt_n\int_0^t dt_{n+1}...$$

$$\int_0^\infty\prod_{k=1}^{N}[-\frac{dS_1(t_k|x_{\pi(k),0},1,L)}{dt_k}]dt_n$$

$$=S(t|x_1^0,1,L)...S(t|x_n^0,1,L)(1-S(t|x_{n+1}^0,1,L))(1-S(t|x_N^0,1,L)),$$

where the combinatorial factors arise as a consequence of the particles exchange symmetry discussed in presenting the Reflection Principle Method. In fact, as particles are independent, we do not know a priori which one exits and which one survives, and we have to consider all the possibilities, i.e. all the permutations of the N indexes. To our purpose, the temporal order of the exit events is irrelevant; permutations inside the same set on $N-n$ indexes are equivalent and we have to divide by the number on these permutations. The same reasoning holds for the n particles still inside the channel interval $[-L/2, L/2]$ giving

$$p_n(t|x_0, N, L) = \frac{1}{n!(N-n)!} \sum_{\pi \in \Pi_N} \prod_{k=1}^{n} S_1(t|x_{\pi(k),0}, 1, L) \prod_{k=n+1}^{N} [1 - S_1(t|x_{\pi(k),0}, 1, L)]. \tag{2.10}$$

If the of initial position x_0 for all particles are randomly distributed along the channel, the previous formula simplifies as follows:

$$p_n(t|N, L) = \binom{N}{k} S_1(t|1, L)^k [1 - S_1(t|1, L)]^{N-k}. \tag{2.11}$$

We then obtain the following form for the Survival Probability

$$S_n(t|N, L) = \sum_{k=n}^{N} \binom{N}{k} S_1(t|1, L)^k [1 - S_1(t|1, L)]^{N-k}, \tag{2.12}$$

where

$$S_1(t|1, L) := \frac{1}{L} \int_{-L/2}^{L/2} S_1(t|x_k^0, 1, L) dx_k^0 \tag{2.13}$$

is the Survival Probability of a free particle initially placed at random position within the channel. Interest in $S_n(t|N, L)$ arises since such function is the one which govern the escape dynamics of particles in Single File. In particular the channel emptying probability becomes:

$$\begin{aligned} 1 - S_1(t|N, L) &= 1 - \sum_{k=1}^{N} \binom{N}{k} S_1(t|1, L)^k [1 - S_1(t|1, L)]^{N-k} = \\ &= 1 - \sum_{k=0}^{N} \binom{N}{k} S_1(t|1, L)^K [1 - S_1(t|1, L)]^{N-k} + \\ &+ \binom{N}{0} S_i(t|1, L)^0 [1 - S_1(t|1, L)]^N = \\ &= 1 - (S_1(t|1, L) + 1 - S_1(t|1, L))^N + (1 - S_1(t|1, L))^N = \\ &= [1 - S_1(t|1, L)]^N. \end{aligned} \tag{2.14}$$

2.3 Survival Probability of a Single Brownian particle

In this section we will present an analytical derivation of the fundamental quantities needed for the description of diffusive motion of a single Brownian particle. Being interested in the description of the emptying process, the characteristic function we aim to evaluate are the Survival probability for a single Brownian particle $S_1(t|x^0, 1, L)$ and the Mean First Passage Time $T(x^0, 1, L)$ which will be calculated as an estimate of the first time in which the particle under exam reaches the absorbing boundary, i.e. is expelled from the channel system. We will evaluate these two quantities in three different forms:

- the more general one with dependence on initial condition;
- the case of defined initial conditions as uniformly distributed between $[-L/2, L/2]$;
- the case of defined initial conditions as uniformly distributed between $[-L_0/2.L_0/2]$ where $L_0 < L$.

In this section we will focus on the simplest case of absence of an external force F_e. The dynamics of the system can be studied by calculating the probability distribution function $p_1(x, t|x_0, 1, L)$ solving:

$$\frac{\partial p_1(x,t|x_0,1,L)}{\partial t} = D\frac{\partial^2 p_1(x,t|x_0,1,L)}{\partial^2 x}. \tag{2.15}$$

In order to find a solution for the previous equation, we can use the standard method of separation of variables writing the function in exam as

$$p_1(x,t|x_0) = X(x)T(t). \tag{2.16}$$

Thus, we can now focus on solving two separate equations:

$$\begin{cases} \frac{T'(t)}{T(t)} = -D_t\lambda^2 \\ \\ X''(x) = -\lambda^2 X(x). \end{cases} \tag{2.17}$$

Globally we will have

$$\begin{aligned} p(x,t|x_0,0) = X(x)T(t) = \\ \\ = (A_\lambda \sin(\lambda x) + B_\lambda \cos(\lambda x))e^{D\lambda^2 t}, \end{aligned} \tag{2.18}$$

where the constants A and B have to be evaluated by imposing the boundary conditions chosen for this analysis, in our case absorbing ones. Let's now introduce the absorbing

boundary conditions at the positions $x = b_1$ and $x = b_2$, remembering that $b_2 - b_1 = L$. This choice of boundary conditions implies that

$$p_1(L, t|x_0) = 0 \tag{2.19}$$

By imposing such constriction we derive that it is necessary that $B_\lambda = 0$ and

$$\sin(\lambda L) = 0 \longleftrightarrow \lambda = \frac{n\pi}{L} \; \forall n \in \mathbb{Z} \tag{2.20}$$

This gives

$$p_1(x, t|x_0) = \sum_n A_n \sin(\frac{n\pi}{L}(x + \frac{L}{2}))e^{-D_t \frac{n^2\pi^2}{L^2}t}. \tag{2.21}$$

In order to find an expression for the coefficients A_n let's impose the following initial condition:

$$p_1(x, t \longrightarrow 0|x_0) = \delta(x - x_0). \tag{2.22}$$

To find A_n we have to invert the Fourier Series, using the correct orthonormal base

$$\begin{aligned} A_n &= \frac{2}{L}\int_0^L \sin(\frac{n\pi}{L}(x + \frac{L}{2}))\delta(x - x_0) = \\ &= \frac{2}{L}\sin(\frac{n\pi}{L}(x_0 + \frac{L}{2})). \end{aligned} \tag{2.23}$$

Inserting now the expression for A_n into equation (2.18) we finally obtain the probability distribution function for a free single Brownian particle in presence of absorbing boundaries:

$$p_1(x, t|x_0, 1, L) = \frac{2}{L}\sum_{n=0}^{\infty} \sin\left(\frac{n\pi(x + L/2)}{L}\right) \sin\left(\frac{n\pi(x_0 + L/2)}{L}\right) e^{-D(\frac{n\pi}{L})^2 t}. \tag{2.24}$$

By integrating this function we get the Survival Probability:

$$S_1(t|x_0,1,L) = \frac{2}{L}\sum_n \sin\left(\frac{n\pi(x_0+L/2)}{L}\right) e^{-\frac{Dn^2(2n+1)^2\pi^2 t}{L^2}} \int_{-\frac{L}{2}}^{\frac{L}{2}} \sin\left(\frac{n\pi(x+L/2)}{L}\right) dx = \tag{2.25}$$

$$= \frac{2}{L}\sum_n \sin\left(\frac{n\pi(x_0+L/2)}{L}\right) e^{-\frac{Dn^2(2n+1)^2\pi^2 t}{L^2}} \int \frac{L}{n\pi}\sin(x')dx' =$$
$$= -\frac{2}{L}\sum_n \sin\left(\frac{n\pi(x_0+L/2)}{L}\right) e^{-\frac{Dn^2(2n+1)^2\pi^2 t}{L^2}} [\cos(n\pi)-1] =$$
$$= \frac{4}{\pi}\sum_n \frac{1}{(2n+1)}\sin\left(\frac{(2n+1)\pi(x_0+L/2)}{L}\right) e^{-\frac{Dn^2(2n+1)^2\pi^2 t}{L^2}},$$

where $x' = \frac{n\pi}{L}(x+L/2)$, and the last passage is justified because the bracket $[\cos(n\pi)-1]$ can have the values 0 if n is even, and -1 if n is odd. So in the cases of even n, the function is zero. We can than eliminate the even term by substituting n with $2n+1$. Our interest in the study of the emptying process leads us to evaluate also the Mean First Passage Time since this quantity represents the time in which the particle under exam exits from the channel system. By integrating the Survival Probability (2.25) over time we will have:

$$T(x_0|1,L) = \frac{4}{\pi^3}\sum_n \frac{L^2}{(2n+1)^3 D^2}\sin\left(\frac{\pi(2n+1)(x_0+L/2).}{L}\right) \tag{2.26}$$

The next step is to eliminate the dependence of the Survival Probability from the initial position x_0 by assigning a general initial distribution for all particles. Let's consider all particles initially uniformly distributed between $[-L/2, L/2]$. By integrating (2.25) over such uniform distribution we get:

$$S_1(t|1,L) = \frac{4}{\pi}\sum_n \frac{1}{(2n+1)} e^{-\frac{Dn^2(2n+1)^2\pi^2 t}{L^2}} \frac{1}{L}\int_{-\frac{L}{2}}^{\frac{L}{2}} \sin\left(\frac{(2n+1)\pi(x_0+L/2)}{L}\right) dx_0 = \tag{2.27}$$

$$= \frac{4}{\pi}\sum_n \frac{1}{(2n+1)} e^{-\frac{Dn^2(2n+1)^2\pi^2 t}{L^2}} \frac{1}{L}\int \frac{L}{(2n+1)\pi}\sin(x_1) =$$
$$= -\frac{4}{\pi}\sum_n \frac{1}{(2n+1)} e^{-\frac{Dn^2(2n+1)^2\pi^2 t}{L^2}} \frac{1}{L}\frac{L}{(2n+1)\pi}[\cos((2n+1)\pi)-1] =$$
$$= \frac{8}{\pi^2}\sum_n \frac{1}{(2n+1)^2} e^{-\frac{Dn^2(2n+1)^2\pi^2 t}{L^2}},$$

where $x_1 = (2n+1)\pi\frac{x_0+L/2}{L}$. Finally by integrating the Survival Probability $S(t|1,L)$ over time, we can obtain the Mean First Passage Time for the single particle as follows:

$$\begin{aligned} T(1,L) &= \int_0^\infty S(t)dt = \\ &= \frac{8}{\pi^2}\sum_n \frac{1}{(2n+1)^2}\int_0^\infty e^{-\frac{Dn^2(2n+1)^2\pi^2 t}{L^2}}dt = \\ &= \frac{8}{\pi^4}\sum_n \frac{L^2}{(2n+1)^4 D_t^2}. \end{aligned} \tag{2.28}$$

As we can see, the Mean First Passage Time shows a dependence on L^2, thus increasing rapidly with the growing of the channel length L. A more general case, in which all particles are initially uniformly distributed in a region defined by the interval $[-\frac{L_0}{2}, \frac{L_0}{2}]$ where $L_0 < L$ can be also computed. In this case the integration has to be performed with the new extremes giving:

$$\begin{aligned} S_1(t|1,L,L_0) &= \frac{4}{\pi}\sum_n \frac{1}{(2n+1)}e^{-\frac{Dn^2(2n+1)^2\pi^2 t}{L^2}}\frac{1}{L_0}\int_{-\frac{L_0}{2}}^{\frac{L_0}{2}} \sin\left(\frac{(2n+1)\pi(x_0+L/2)}{L}\right)dx_0 = \\ &= \frac{4}{\pi}\sum_n \frac{1}{(2n+1)}e^{-\frac{Dn^2(2n+1)^2\pi^2 t}{L^2}}\frac{1}{L_0}\int \frac{L}{(2n+1)\pi}\sin(x_1) = \\ &= \frac{L}{L_0}\frac{4}{\pi}\sum_n \frac{1}{(2n+1)}e^{-\frac{Dn^2(2n+1)^2\pi^2 t}{L^2}}\frac{1}{(2n+1)\pi} \\ &\left[\cos\left(\frac{(2n+1)\pi(L-L_0)}{2L}\right) - \cos\left(\frac{(2n+1)\pi(L_0+L)}{2L}\right)\right], \end{aligned} \tag{2.29}$$

where $x_1 = \frac{(2n+1)\pi(x_0+L/2)}{L}$. Hence

$$T(1,L,L_0) = \int_0^\infty S(t)dt =$$

$$= \frac{L}{L_0}\frac{4}{\pi^2}\sum_n \frac{1}{(2n+1)^2}\left[\cos\left(\frac{(2n+1)\pi(L-L_0)}{2L}\right) - \cos\left(\frac{(2n+1)\pi(L_0+L)}{2L}\right)\right].$$

$$\int_0^\infty e^{-\frac{Dn^2(2n+1)^2\pi^2 t}{L^2}}dt =$$

$$= \frac{L^3}{L_0}\frac{4}{\pi^4}\sum_n \frac{1}{D_t^2(2n+1)^4}\left[\cos\left(\frac{(2n+1)\pi(L-L_0)}{2L}\right) - \cos\left(\frac{(2n+1)\pi(L_0+L)}{2L}\right)\right]. \tag{2.30}$$

As we can see, equation (2.29) reduced to (2.27) in case of $L = L_0$ as we should have expected.

2.3.1 Presence of an external force

In this section we will consider the more general case of a Single File in presence of a external force F_e assumed to be constant and uniform. The idea is to apply again the argument introduced in the previous section and use the Survival Probability for a single forced Brownian particle as building block for our calculations. This can be done, in principle, for any value of the external bias F_e. Indeed, in the presence of a strong force, particles are dragged along one direction and substantially do not interact with each other. The order is still preserved, particles are equal and perform elastic collisions, thus the Reflection Principle Method previously discussed is safely applicable. To calculate the Survival Probability, as well as the Mean First Passage time, we will follow the same path as in the previous section and derive the analytical expressions for the Survival Probability and for the Mean First Passage time in three different forms:

- the more general one with dependence on initial condition;
- the case of defined initial conditions as uniformly distributed between $[-L/2, L/2]$;
- the case of defined initial conditions as uniformly distributed between $[-L_0/2.L_0/2]$ where $L_0 < L$.

By working under the Overdameped limit, we start from the Langevin equation (1.4) with the additional force term F_e.

$$\frac{dx(t)}{dt} = \frac{Fe}{m\gamma} + f(t), \tag{2.31}$$

where $f(t)$ is the Gaussian noise defined as in section 1. To equation (2.31) corresponds the Fokker-Planck one [19] for the conditional probability $p_1(x, t, |x_0, 1, L, \Gamma)$:

$$\frac{\partial}{\partial t} p_1(x, t|x_0, 1, L, \Gamma) = -\frac{Fe}{m\gamma}\frac{\partial}{\partial x} p_1(x, t|x_0, 1, L, \Gamma) + D_t \frac{\partial^2}{\partial^2 x} p_1(x, t|x_0, 1, L, \Gamma), \tag{2.32}$$

where $\Gamma = \frac{Fe}{2m\gamma D_t}$. By factorizing the spatial and temporal dependence as $p_1(x, t|x_0, 1, L, \Gamma) = X(x)T(t)$l,, equation (2.32) becomes:

$$D_t^{-1}\frac{T'(t)}{T(t)} = -2\Gamma\frac{X'(x)}{X(x)} := -\lambda^2 \ . \tag{2.33}$$

By solving each equation separately we finally get

$$p_1(x, t|x_0, 1, L, \Gamma) = (A_\lambda \cos(1/2\sqrt{4\lambda^2 - 4\Gamma^2 x}) + B_\lambda \sin(1/2\sqrt{4\lambda^2 - 4\Gamma^2 x}))e^{-\lambda^2 Dt}. \tag{2.34}$$

The constants A_λ and B_λ have to be calculated by imposing the absorbing boundary conditions at the channel ends b_1 and b_2, i.e. $p_1(b_1, t|x_0, 1, L) = 0$ and $p_1(b_2, t|x_0, 1, L) = 0$.

These imply $A_\lambda = 0$ so that we have only to impose:

$$\sin(\frac{1}{2}\sqrt{4\lambda^2 - 4\Gamma^2}L*) = 0 \longleftrightarrow \lambda = \sqrt{(\frac{n\pi}{L*})^2 + \Gamma^2}. \tag{2.35}$$

Solution (2.34) must also satisfy the initial condition

$$p(x, t \longrightarrow 0|x_0, 1, L, \Gamma) = \sum_n A_n e^{\Gamma x} \sin(\frac{n\pi}{L}x) = \delta(x - x_0). \tag{2.36}$$

In order to find the coefficient A_n we use the Fourier series as follows:

$$\begin{aligned} A_n &= \frac{2}{L}\int_0^L e^{\Gamma z} \sin(\frac{n\pi}{L}z)\delta(z - z_0)dz \\ &= \frac{2}{L}e^{\Gamma z_0} \sin(\frac{n\pi}{L}z_0). \end{aligned} \tag{2.37}$$

By inserting $b_1 = -\frac{L}{2}$ and $b_2 = \frac{L}{2}$ we finally get

$$p(x, t|x_0, 1, L, \Gamma) = \frac{2}{L}\sum_n e^{\Gamma(x+\frac{L}{2})}e^{-\Gamma(x_0+\frac{L}{2})} \sin(\frac{n\pi}{L}(x+\frac{L}{2})) \sin(\frac{n\pi}{L}(x_0+\frac{L}{2}))e^{-D_t[(\frac{n\pi}{L})^2+\Gamma^2]t}. \tag{2.38}$$

We are now able to compute the Survival Probability by integrating (2.38) between $-\frac{L}{2}$ and $\frac{L}{2}$. In order to simplify the calculation let's evaluate first the following integral:

$$\begin{aligned} &\int_{-\frac{L}{2}}^{\frac{L}{2}} e^{\Gamma x} \sin\left(\frac{n\pi}{L}(x + \tfrac{L}{2})\right) dx = \\ &= \frac{1}{\Gamma}e^{\Gamma x} \sin\left(\frac{n\pi}{L}(x + \tfrac{L}{2})\right)\Big|_{L/2}^{L/2} - \frac{1}{\Gamma}\int_{-\frac{L}{2}}^{\frac{L}{2}} e^{\Gamma x} \cos\left(\frac{n\pi}{L}(x + \tfrac{L}{2})\right) \frac{n\pi}{L}dx = \\ &= -\frac{1}{\Gamma}\left[\frac{1}{\Gamma}e^{\Gamma x} \cos\left(\frac{n\pi}{L}(x + \tfrac{L}{2})\right) \frac{n\pi}{L}\Big|_{L/2}^{L/2} + \frac{1}{\Gamma}\int_{-\frac{L}{2}}^{\frac{L}{2}} e^{\Gamma x} \sin\left(\frac{n\pi}{L}(x + \tfrac{L}{2})\right) \left(\frac{n\pi}{L}\right)^2 dx\right] = \\ &= -\frac{1}{\Gamma^2}e^{\Gamma L/2} \cos(n\pi)\frac{n\pi}{L} + \frac{1}{\Gamma^2}\frac{n\pi}{L}e^{-\Gamma L/2} - (\frac{n\pi}{\Gamma L})^2\int_{-\frac{L}{2}}^{\frac{L}{2}} e^{\Gamma x} \sin\left(\frac{n\pi}{L}(x + \tfrac{L}{2})\right) dx, \end{aligned} \tag{2.39}$$

giving

$$\int_{-\frac{L}{2}}^{\frac{L}{2}} e^{\Gamma x} \sin\left(\frac{n\pi}{L}(x+\tfrac{L}{2})\right) dx \left(1+(\frac{n\pi}{L\Gamma})^2\right) = \tag{2.40}$$

$$\tag{2.41}$$

$$= \frac{(n\pi/L\Gamma^2)e^{\Gamma L/2}(1-e^{\Gamma L}\cos(n\pi))}{1+(n\pi/L\Gamma)^2} =$$

$$\tag{2.42}$$

$$= \frac{Ln\pi e^{-\Gamma L/2}(1-e^{\Gamma L}\cos(n\pi))}{(n\pi)^2+(L\Gamma)^2}.$$

Hence

$$\int_{-\frac{L}{2}}^{\frac{L}{2}} e^{\Gamma(x+L/2)} \sin\left(\frac{n\pi}{L}(x+\tfrac{L}{2})\right) dx \left(1+(\frac{n\pi}{L\Gamma})^2\right) = \tag{2.43}$$

$$\tag{2.44}$$

$$= \frac{Ln\pi(1-e^{\Gamma L}\cos(n\pi))}{(n\pi)^2+(L\Gamma)^2}.$$

Finally we get

$$\begin{aligned} S(t|x_0,1,L,\Gamma) = \frac{2}{L}\sum_n e^{-\Gamma(x_0+L/2)} \sin\left(\frac{n\pi}{L}(x_0+\tfrac{L}{2})\right) e^{-D_t[(\frac{n\pi}{L})^2+\Gamma^2]t}. \\ \int_{-\frac{L}{2}}^{\frac{L}{2}} e^{\Gamma(x+L/2)} \sin\left(\frac{n\pi}{L}(x+\tfrac{L}{2})\right) dx = \\ = \frac{2}{L}\sum_n e^{-\Gamma(x_0+L/2)} \sin\left(\frac{n\pi}{L}(x_0+\tfrac{L}{2})\right) e^{-D_t[(\frac{n\pi}{L})^2+\Gamma^2]t} \\ \frac{n\pi(1-e^{-\Gamma L}\cos(n\pi))}{(n\pi)^2+(L\Gamma)^2}. \end{aligned} \tag{2.45}$$

2.3.2 Uniform initial distribution within $[-\frac{L}{2}, \frac{L}{2}]$

Let's now focus on the particles initial distribution. We first choose the particles uniformly distributed within the interval $[-\frac{L}{2}, \frac{L}{2}]$. By integrating over the initial distribution we obtain:

$$\begin{aligned} S(t|1,L,\Gamma) = \int S(t|x_0,1,L,\Gamma)p(x_0)dx_0 = \\ = \frac{1}{L}\int_{-\frac{L}{2}}^{\frac{L}{2}} S(t|x_0\Gamma,)dx_0, \end{aligned} \tag{2.46}$$

where $p(x_0)$ is the uniform distribution function. In analogy with what we did before, considering only the part of $p(x,t|x_0,1,L)$ that depends on the initial condition x_0 the integral gives:

$$\begin{aligned}&\frac{1}{L}\int_{-\frac{L}{2}}^{\frac{L}{2}} e^{-\Gamma(x_0+L/2)}\sin\left(\frac{n\pi}{L}(x_0+\tfrac{L}{2})\right)dx_0 = \\ &= \frac{n\pi(1-e^{-\Gamma L}\cos(n\pi))}{(n\pi)^2+(L\Gamma)^2}.\end{aligned} \tag{2.47}$$

Hence

$$S(t|1,L,\Gamma) = 2\sum_n \frac{(n\pi)^2(1-e^{\Gamma L}\cos(n\pi)(1-e^{-\Gamma L}\cos(n\pi))}{[(\Gamma L)^2+(n\pi)^2]^2}e^{-D_t[(\frac{n\pi}{L})^2+\Gamma^2]t}. \tag{2.48}$$

From equation (2.48) we can derive the Mean First Time Passage of the single particle by simply integrating over time. This gives

$$\begin{aligned}T(1,L) &= \int_0^\infty S(t)dt = \\ &= 2\sum_n \frac{(n\pi)^2(1-e^{\Gamma L}\cos(n\pi)(1-e^{-\Gamma L}\cos(n\pi))}{[(\Gamma L)^2+(n\pi)^2]^2}\int_0^\infty e^{-D_t[(\frac{n\pi}{L})^2+\Gamma^2]t}dt = \\ &= 2L^2\sum_n \frac{(n\pi)^2(1-e^{\Gamma L}\cos(n\pi)(1-e^{-\Gamma L}\cos(n\pi))}{D_t[(\Gamma L)^2+(n\pi)^2]^3}.\end{aligned} \tag{2.49}$$

In Figure 2.2 we can see the dependence of Equation (2.49) on the channel length and on the coefficient Γ

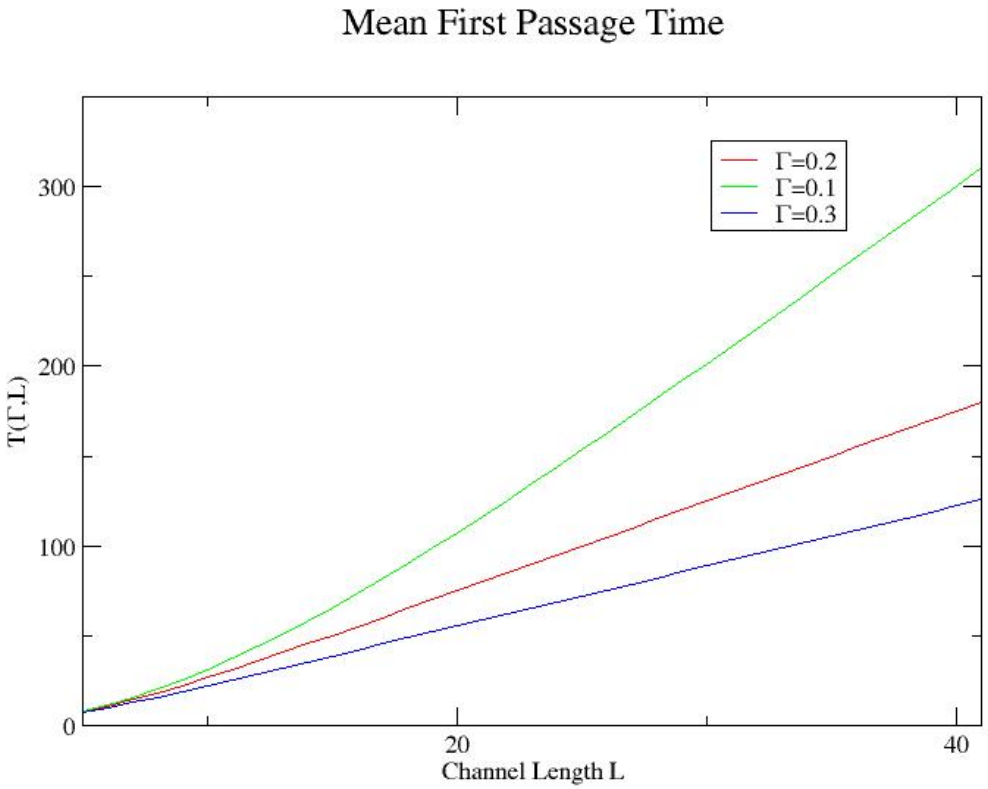

Figure 2.2: Mean First Passage Time as a function of the channel length L for three fixed values of Γ.

As a function of L, the Mean First Passage Time shows a linear behavior, in contrast with the L^2 behavior typical of a Brownian particle as we have seen in equation (2.28). On the other side, for increasing values of the coefficient Γ, the Mean Emptying Time decreases.

2.3.3 Uniform initial distribution within $[-\frac{L_0}{2}, \frac{L_0}{2}]$

Let us suppose now that particles are still uniformly distributed but within the interval $[\frac{L_0}{2}, \frac{L_0}{2}]$ with $L_0 < L$. In this case we have

$$\begin{aligned}
&\int_{-\frac{L_0}{2}}^{\frac{L_0}{2}} e^{-\Gamma(x_0+\frac{L}{2})} \sin\left(\frac{n\pi}{L}(x_0+\tfrac{L}{2})\right) dx_0 = \qquad (2.50)\\
&= e^{-\Gamma L/2}\left[-\frac{1}{\Gamma}e^{-\Gamma L_0/2}\sin\left(\frac{n\pi}{2L}(L_0+L)\right)+\frac{1}{\Gamma}e^{\Gamma L_0/2}\sin\left(\frac{n\pi}{2L}(L-L_0)\right)\right.\\
&\left.+\frac{1}{\Gamma}\int_{-\frac{L_0}{2}}^{\frac{L_0}{2}} e^{-\Gamma x_0}\cos\left(\frac{n\pi}{L}(x_0+\frac{L}{2})\right)\frac{n\pi}{L}\right] dx_0 =\\
&= e^{-\Gamma L/2}\left[-\frac{1}{\Gamma}e^{-\Gamma L_0/2}\sin\left(\frac{n\pi}{2L}(L_0+L)\right)+\frac{1}{\Gamma}e^{\Gamma L_0/2}\sin\left(\frac{n\pi}{2L}(L-L_0)\right)\right.\\
&-\frac{1}{\Gamma^2}e^{-\Gamma L_0/2}\cos\left(\frac{n\pi}{2L}(L_0+L)\right)\frac{n\pi}{L}+\frac{1}{\Gamma^2}e^{\Gamma L_0/2}\cos\left(\frac{n\pi}{2L}(L-L_0)\right)\frac{n\pi}{L}\\
&\left.+\int_{-\frac{L_0}{2}}^{\frac{L_0}{2}} e^{-\Gamma x_0}\sin\left(\frac{n\pi}{L}(x_0+\tfrac{L}{2})\right)\left(\frac{n\pi}{\Gamma L}\right)^2 dx_0\right].
\end{aligned}$$

By moving the last integral to the left side of the equation we obtain:

$$\begin{aligned}
&\left(1+\left(\frac{n\pi}{\Gamma L}\right)^2\right)\int_{-\frac{L_0}{2}}^{\frac{L_0}{2}} e^{-\Gamma(x_0+\frac{L}{2})}\sin\left(\frac{n\pi}{L}(x_0+\tfrac{L}{2})\right)dx_0 = \qquad (2.51)\\
&= e^{-\Gamma L/2}\left[-\frac{1}{\Gamma}e^{-\Gamma L_0/2}\sin\left(\frac{n\pi}{2L}(L_0+L)\right)+\frac{1}{\Gamma}e^{\Gamma L_0/2}\sin\left(\frac{n\pi}{2L}(L-L_0)\right)\right.\\
&\left.-\frac{1}{\Gamma^2}e^{-\Gamma L_0/2}\cos\left(\frac{n\pi}{2L}(L_0+L)\right)\frac{n\pi}{L}+\frac{1}{\Gamma^2}e^{\Gamma L_0/2}\cos\left(\frac{n\pi}{2L}(L-L_0)\right)\frac{n\pi}{L}\right],
\end{aligned}$$

giving

$$\begin{aligned}
S(t|1,L,L_0,\Gamma) = \frac{2L}{L_0}\sum_n (n\pi)\frac{1-e^{\Gamma L}\cos(n\pi)}{((\Gamma L)^2+(n\pi)^2)^2}\left[e^{-\Gamma(L-L_0)/2}[\Gamma L\sin(\frac{n\pi(L-L_0)}{2L})+n\pi\cos(\frac{n\pi(L-L_0)}{2L})]+\right.\\
\left.-\ e^{-\Gamma(L+L_0)/2}[\Gamma L\sin(\frac{n\pi(L+L_0)}{2L})+n\pi\cos(\frac{n\pi(L+L_0)}{2L})]\right]e^{-D_t[(\frac{n\pi}{L})^2+\Gamma^2]t}. \qquad (2.52)
\end{aligned}$$

As done previously, from this expression of $S(t|1,L,L_0,\Gamma)$ one can derive the Mean

First Passage Time by integrating $S(t|1, L, L_0, \Gamma)$ over time , obtaining the following result:

$$
\begin{aligned}
T(1, L, L_0, \Gamma) &= \int_0^\infty S(t|1, L, L_0, \Gamma)dt = \\
&= \frac{2L}{L_0}\sum_n (n\pi)\frac{1 - e^{\Gamma L}\cos(n\pi)}{((\Gamma L)^2 + (n\pi)^2)^2}\Big[e^{-\Gamma(L-L_0)/2}[\Gamma L \sin(\frac{n\pi(L - L_0)}{2L}) + \\
&+ n\pi\cos(\frac{n\pi(L - L_0)}{2L})] - e^{-\Gamma(L+L_0)/2}[\Gamma L \sin(\frac{n\pi(L + L_0)}{2L}) + \\
&+ n\pi\cos(\frac{n\pi(L + L_0)}{2L})]\Big]\int_0^\infty e^{-D_t[(\frac{n\pi}{L})^2+\Gamma^2]t}dt = \\
&= \frac{2L^3}{L_0}\sum_n (n\pi)\frac{1 - e^{\Gamma L}\cos(n\pi)}{D_t((\Gamma L)^2 + (n\pi)^2)^3}\Big[e^{-\Gamma(L-L_0)/2}[\Gamma L \sin(\frac{n\pi(L - L_0)}{2L}) + \\
&+ n\pi\cos(\frac{n\pi(L - L_0)}{2L})] - e^{-\Gamma(L+L_0)/2}[\Gamma L \sin(\frac{n\pi(L + L_0)}{2L}) + n\pi\cos(\frac{n\pi(L + L_0)}{2L})]\Big].
\end{aligned}
\tag{2.53}
$$

By comparing (2.53) and (2.49) we can see that, for a fixed value of the coefficient Γ, the Mean First Passage Time at the absorbing boundary is higher if the particle has an initial condition uniformly distributed within the interval $[-L_0/2, L_0/2]$. Furthermore, we can notice that (2.53) reduces to (2.49) if we set $L = L_0$ as we would have expected.

2.4 Numerical simulation: emptying times

In this section we present a numerical study of the emptying process. In particular we would like to compare the numerical findings with the analytical solution found in previous sections for $S(t|1, L)$ and $T(1, L)$ sections we have found analytical solution for the Survival Probability density function and for the Mean First Passage, thus we would like compare them with the numerical results we derived from simulations.

Such system is integrated numerically using LAMMPS simulator, modeling a channel of length L = 100 (lj units of LAMMPS) which has been filled at the beginning with one atom in order to verify the single particle formula for emptying time (2.26). The absorbing boundaries have been modelized using two cones (of radius r = 50 in lj units) at each end of the cylinder. In this way, if a particle exits from the channel it will be very unlikely that it will enter again. A visual sketch of the system used for the numerical simulations is reported in Figure 2.3, which schematically represents the channel filled with point-like particles:

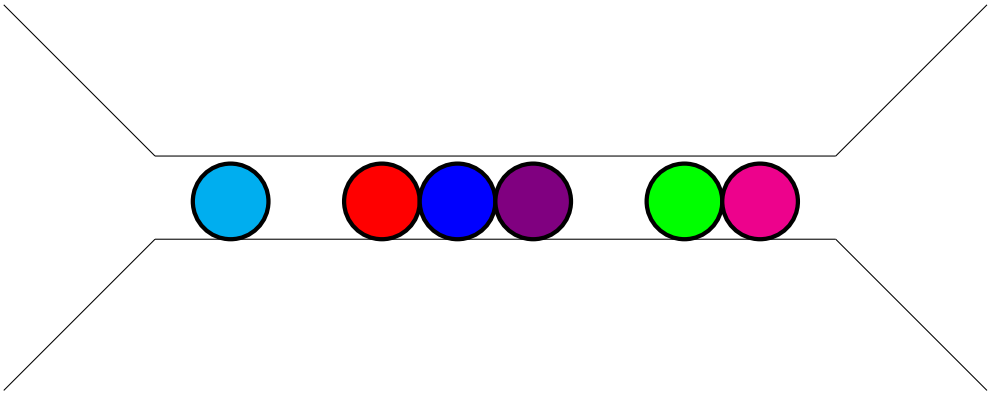

Figure 2.3: Scheme of the channel system used by the numerical simulations with LAMMPS program. The two cones at the channels extremes represent the absorbing boundary conditions, preventing the exiting particles from entering again inside the channel, which has been filled with a single or a group of point-like particles.

2.5 Single point-like particle

First of all, we used the numerical tools previously described in order to study the dynamics of the emptying process of a channel system originally filled with one single particle. We focus on the simplest symmetric case in which the particle is positioned at the center of the channel. We perform 1000 runs with these initial conditions, collecting all the exit times of the particle and then averaging over them. Having calculated the analytical forms for $S(t|x_0, 1, L)$ (2.25) and $T_1(t|x_0, 1, L)$ (2.26) without any approximations, we tested our numerical results by comparing them with the analytical one. Firstly, we numerically evaluate the Mean First Passage Time $T_1(t|x_0, 1, L)$ from simulations obtaining $T(t|x_0, 1, L) = 1164.89$ (lj units) where we chose $x_0 = 0$ as initial position and $L = 100$ (lj units). We calculated also the variance of such mean value and it gave $\sigma = 797.923$ (lj units). As we can see the dispersion of the data is really extended thus generating a too much high value for the variance. Such numerical value has been compared with the

theoretical one evaluated using the formula (2.26) which gave $T = 1250$ (lj units). Taking into consideration the large value of the variance obtained, we can state that the numerical results agree with equation (2.26). In order to justify such big value of the variance we evaluate its statistical properties calculating the second moment of the Probability Distribution Function of the emptying times. Considering that the Mean Emptying Time is defined as in equation (2.26), then it follows that the probability distribution function $\rho(t)$ we have to consider is of the following form:

$$\rho(t|x_0, 1, L) = -\frac{\partial S(t|x_0, 1, L)}{\partial t}, \tag{2.54}$$

where $S(t|x_0, 1, L)$ is the one calculated in equation (2.25). In fact evaluating the mean value of such probability distribution function $\rho(t)$ we obtain the Mean First Passage Time (2.26), which in the case of the emptying process of a channel filled with just one particle corresponds also to the Mean Emptying time. Such mean value can be calculated as follows:

$$\begin{aligned} < t > &= \int_0^\infty -\frac{\partial S(x, t|x_0, 1, L)}{\partial t} t dt = \\ &= -S(x, t|x_0, 1, L)t|_0^\infty + \int_0^\infty S(x, t|)dt = \\ &= T(x_0, 1, L). \end{aligned} \tag{2.55}$$

In order to evaluate the variance of such distribution we first calculated its second moment:

$$\begin{aligned} < t^2 > &= \int_0^\infty -\frac{\partial S(t|x_0, 1, L)}{\partial t} t^2 dt = \\ &= -S(t|x_0, 1, L)t^2|_0^\infty + \int_0^\infty 2S(t|x_0, 1, L)tdt. \end{aligned} \tag{2.56}$$

By plotting numerically the last integral and using the mean value previously calculated we obtain:

$$\sigma = \sqrt{< t^2 > - < t >^2} \sim 1000. \tag{2.57}$$

As we can see, the value of the variance of the considered probability distribution function is quite elevated, thus justifying the numerical one obtained though simulations.

In Figure 2.4 we report the numerical Survival Probability function compared with the analytical one given by equation (2.27):

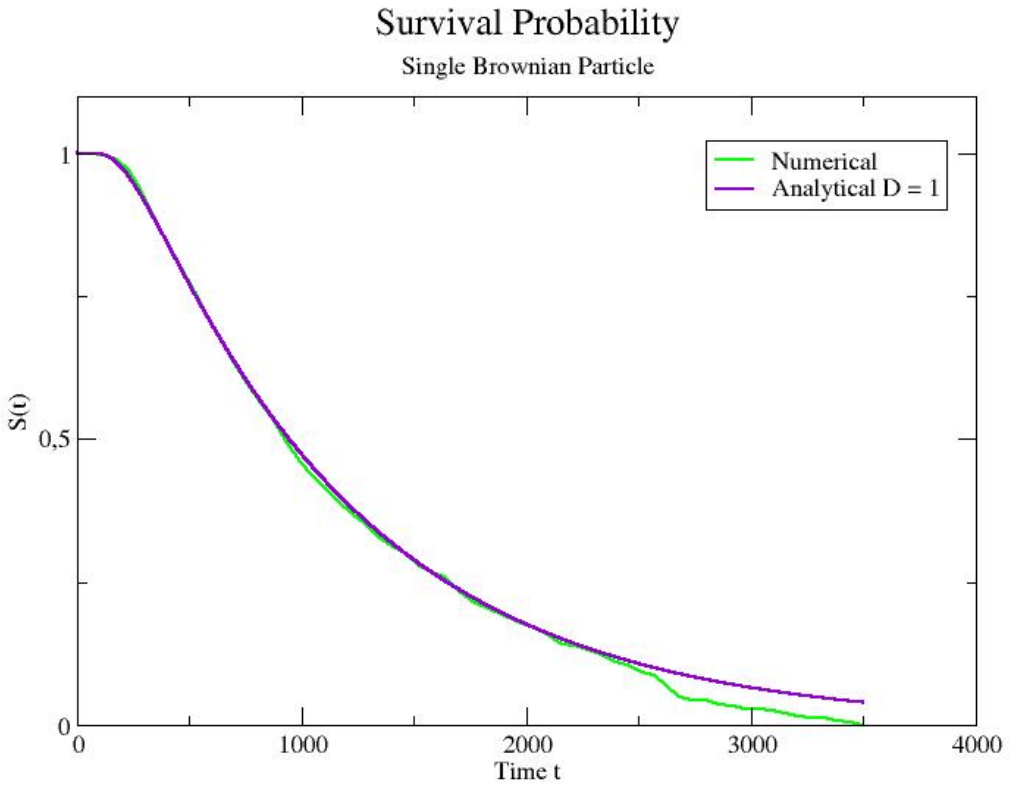

Figure 2.4: Survival Probability over time evolution, analytical and numerical. Such function is calculated building an histogram using the channel emptying times, i.e. the instants when the considered particle exits from the channel.

From Figure 2.4 we can see that the numerical function $S_1(t|x_0, 1, L)$ shows good compatibility with its analytical form. The deviation which can be detected at large times may be attributed to the low statistic which characterize this part of the process. Indeed, the numerical $S_1(t|x_0, 1, L)$ has been built by using histograms of the channel emptying times, thus at higher values of time t few data are available which causes the deviation of $S_1(t|x_0, 1, L)$ from the analytical one.

2.6 Statistics of the emptying process for many point-like particles

Let's now take into consideration a channel filled with 10 particles. In order to begin with a simple analysis we will neglect excluded volume interactions among them. Moreover we assumed that particles are initially uniformly distributed along the channel. As before, the channel of length L = 100 (lj units off LAMMPS) has two cones at the system's extremes in order to represent absorbing boundaries conditions. Because of the absence of volume interactions among particles, we expect to obtain the Survival Probability Function derived in equation (2.12) where $S_1(t|x_0, 1, L)$ represents the Survival Probability of the single particle (2.25). The function $S(t|x_0, 1, L)$ is estimated by working with histograms.

In particular we consider two sets of 500 runs each and evaluate the corresponding $S_1^\alpha(t|x_0,1,L)$ for $\alpha = 1,2$ to evaluate the dispersion of the collected data by plotting the Survival Probability function of each of them separately and observing their difference. In order to get a valuation of the errors associated with the data used to build the histogram, we also take the ratio $\frac{S_1^1}{S_2^2}$ and observe the dispersion of the function obtained from the excepted value of 1 (which would indicate exact compatibility and absence of errors). In Figure 2.5 $S_1^\alpha(t|x_0,1,L)$ with $\alpha = 1,2$ and $\frac{S_1^1}{S_2^2}$ are reported as function of time. We can see the comparison between numerical results for the function $S_1(t|x_0,1,t)$, as well as the evaluation of the dispersion as described before:

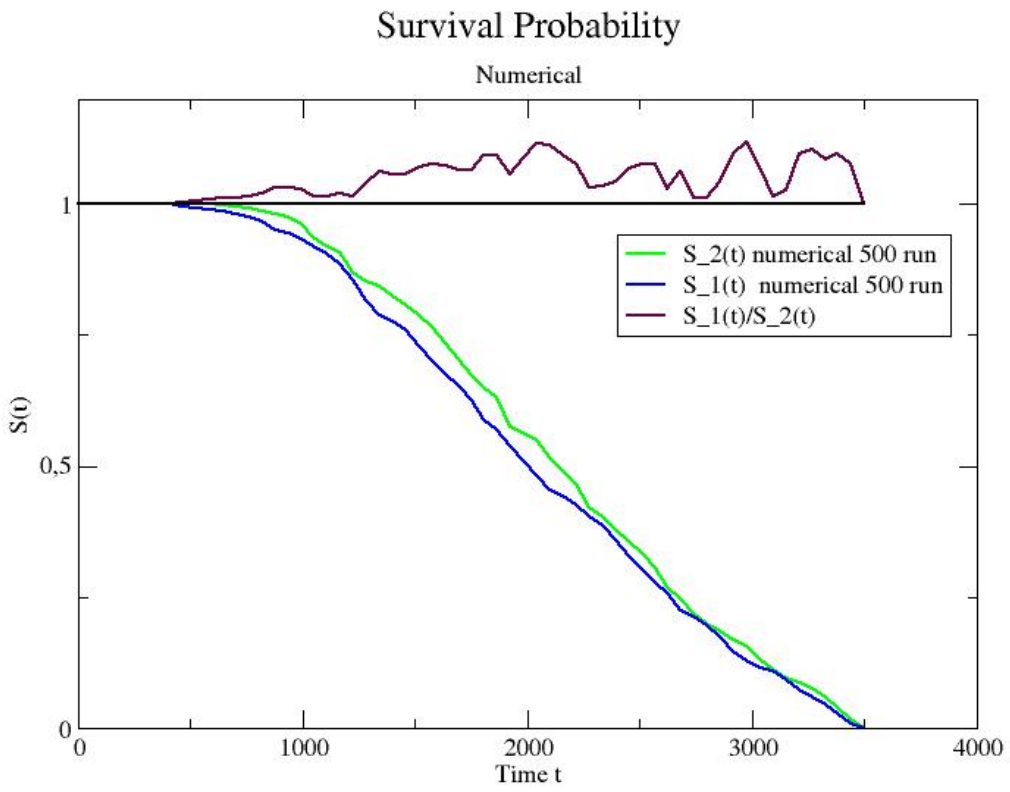

Figure 2.5: Comparison between two Survival Probabilities of single particle derived from two set of 500 runs. The average difference between the two functions obtained represents an estimate of the error related to this numerical function. In the Figure it has also been plotted the ratio $S_1(t)/S_2(t)$ whose fluctuations increase for bigger times.

From Figure 2.5 we can observe how the difference between the two Survival Probability functions increases for bigger values of time t. Such behavior justifies the deviation of the analytical function from the numerical one at larger of t as shown in Figures 2.4 and 2.6. Comparison between the analytical and numerical Survival Probability for a system of many point-like particles can be seen in Figure 2.6 :

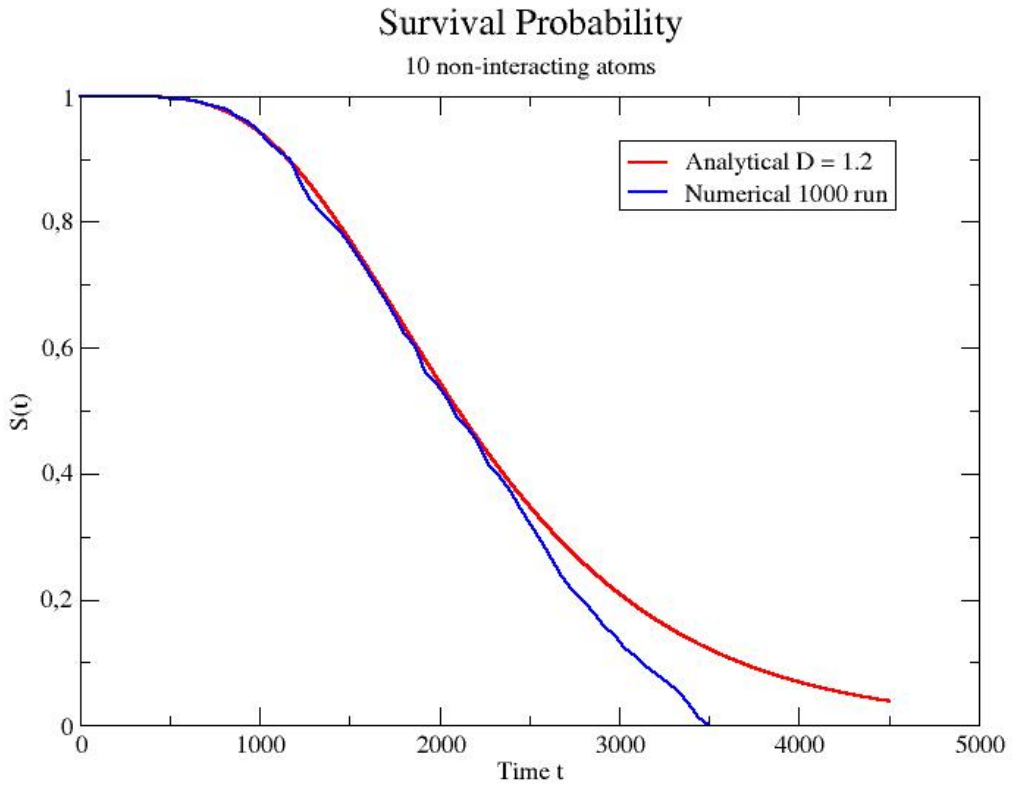

Figure 2.6: Survival Probability over time evolution analytical ((2.25)) and numerical. Such function is calculated building an histogram using the channel emptying times, i.e. the instants when the last particle exits from the channel.

It is also be interesting to look at the dependence of the Survival Probability on the channel length L. In Figure 2.7 we report the Survival Probability as function of time t at four different fixed values of L. This comparison shows that $S_1(t|x_0, 1, L)$ rapidly converges to zero for smaller values of L while decreases more smoothly for increasing values of L.

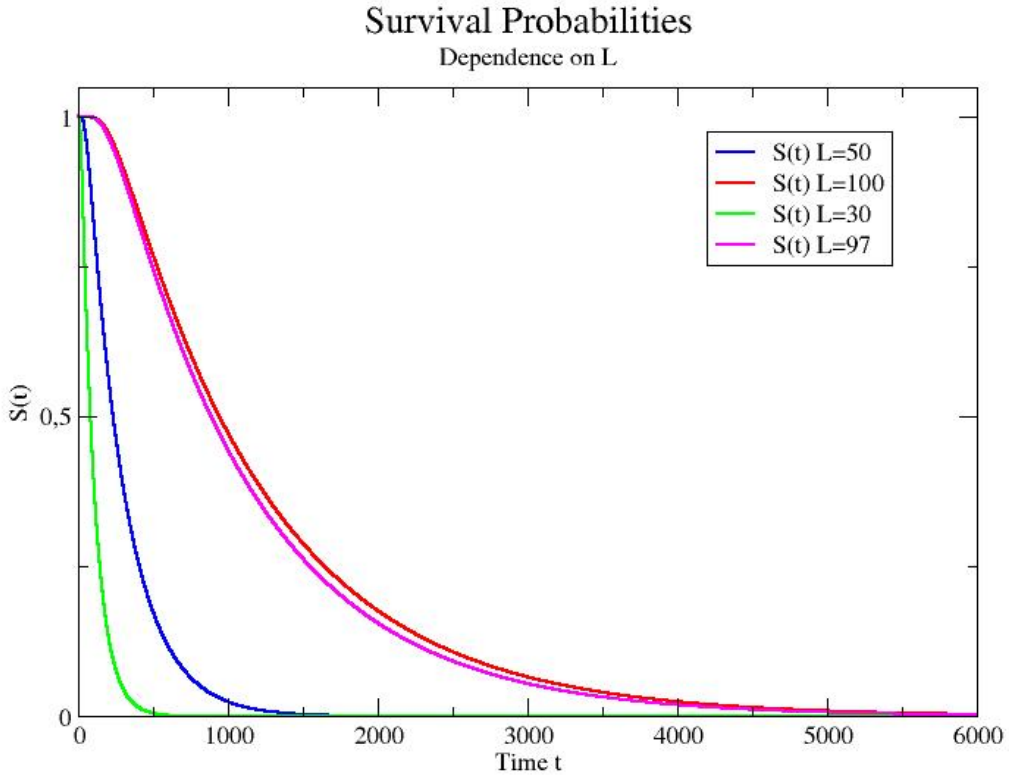

Figure 2.7: Time evolution of Survival Probability for four different fixed values of the channel length L. As we can observe, the shape of the Survival Probability changes accordingly to the value of L converging more rapidly to zero for smaller values of L.

2.6.1 Excluded Volume effects

So far excluded volume interactions among particles have been neglected. The inclusion of these interactions makes the theoretical analysis considerably more difficult and one has to rely either on approximations or on simulations.

Considering the analytical form of the Survival Probability function, the only approach which can be used that take into account the presence of interactions is the introduction of an "effective length", as it will be clearer later in this section. In fact, excluded volume effects of particles of radius R can be taken into account using an effective theory. Remembering the analytical form of the Survival Probability for many non interacting particles

$$S_n(t|N,L) = \sum_{k=n}^{N} \binom{N}{k} S_1(t|1,L)^k [1 - S_1(t|1,L)]^{N-k}, \tag{2.58}$$

we can explicitly derive the Mean First Passage Time of the first $n < N$ particles exiting the channel $T_n(N,L)$ trough the following integral:

$$T_n(N,L) = \int_0^\infty dt S_n(t|N,L). \tag{2.59}$$

Let's now focus on the changes necessary to take into account the interactions at the simplest level of approximations. By considering n particles of radius R (which represent the excluded volume) inside a channel, then its length L reduces to its effective length L

$$L_n = L - 2(n-1)R. \tag{2.60}$$

In order to account for excluded volume effects during exiting process, we can thus define an effective length $L_{eff}(N,L,R)$ through the weighted average:

$$\begin{aligned} L_{eff}(N,L,R) &= \frac{T_N L_N + (T_{N-1} - T_N)L_{N-1} + ... + (T_1 - T_2)L_1}{T_1} = \\ &= \frac{\sum_{k=1}^{N} [T_k(N,L) - T_{k+1}(N,L)](L - 2R(k-1))}{T_1(N,L)}, \end{aligned} \tag{2.61}$$

where $T_{N+1} := 0$. An approximated analytical expression for the Survival Probability function for the system of many particles with volume excluded interactions can be derived by substituting L with L_{eff} derived in equation (2.61) in the expression for $S_n(t|N,L)$ of equation (2.58). We focus only on the numerical aspects of this problem, deriving the Survival Probability function using the same methods as before. The system is the same as the one previously used, i.e. a channel of length $L = 100$ (lj units of LAMMPS) with two cones at the two extremes of it representing the absorbing boundary conditions. Such channel has been now filled with 10 atoms characterized by a Lennard Jones interaction

(cutoff $R_0 = 1.0$, $\sigma = 1.0$) among themselves. Again, through several runs of LAMMPS simulating the dynamic evolution, I collected all emptying times of the channel looking at the exit time of the last particle still inside the system. As I have previously done, in order to build the Survival Probability I created an histogram using the emptying times collected through simulations. The Figure 2.8 shows the numerical results obtained for the Survival Probability function

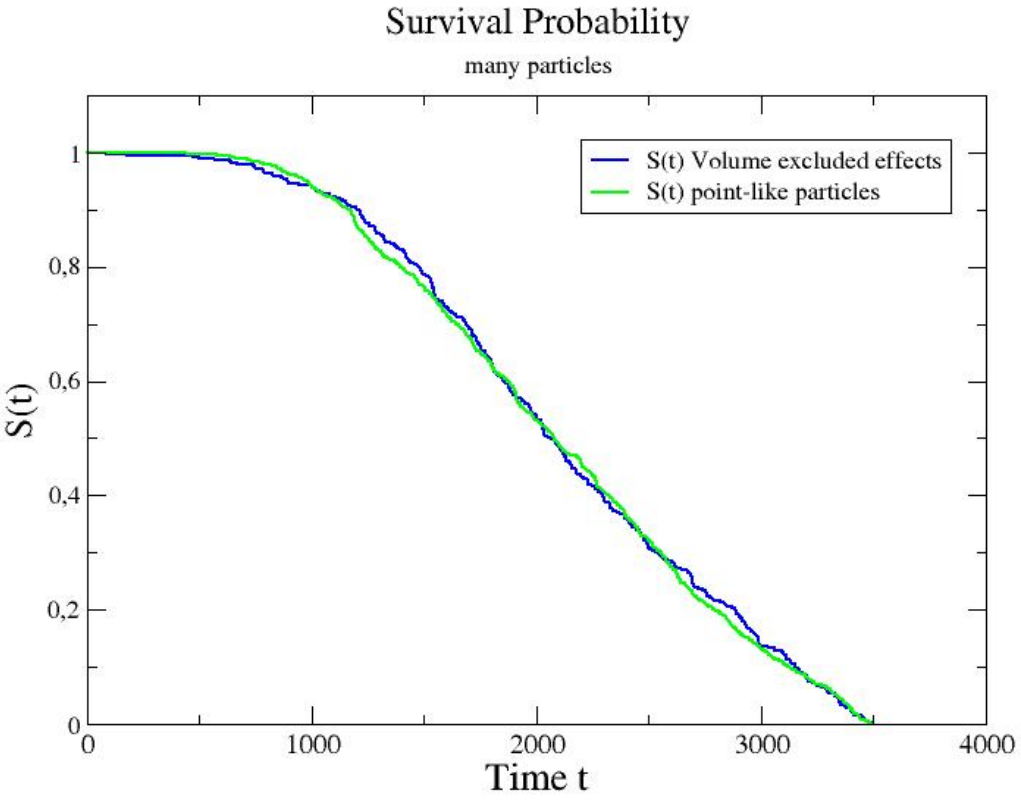

Figure 2.8: Time evolution of the Survival Probability of many interacting particles compared with the one of many point-like particles. These functions are calculated building an histogram using the channel emptying times, i.e. the instants when the last of the 10 interacting particles exits from the channel. The total channel length is $L = 100$ (lj units)

Figure 2.8 shows a comparison between the Survival Probabilities of many particles with volume excluded interactions and the one of many point-like particles. We can see that the shapes of these two functions is approximately identical. From a general point of view, we would have expected to see a faster emptying process in the case of interacting particles, due to the frequent collisions which can led them exit from the channel more quickly. The fact that we do not observe such behavior can be explained by considering that the particles density in the case of volume excluded interactions is probably not high enough to justify it. In this last case indeed, the particles are uniformly distributed along all channel and, after the first ones have quickly exited from it due to the frequent collisions, the remaining particles are too distant from each others to actually feel the effects due to volume excluded interactions.

Chapter 3

Single File Diffusion with partially reflecting boundaries

In this part of the thesis we will consider another kind of boundaries conditions, the Partially Reflecting ones, which can be considered as more appropriate to describe realistic system. Our interest in such boundary conditions relies on the remarkable number of physical systems which can be described using them. Just to cite some examples we can consider interchain reaction of macromolecules, ligand binding to receptors, repressor-operator association of DNA strand [29]. Another peculiar case where Partially Reflecting boundary conditions show great relevance involves the Knots Theory.

The boundary conditions of any stochastic simulation algorithm can be formulated as follows: whenever a molecule hits the boundary, it is absorbed with some probability and reflected otherwise. The special cases of this boundary condition are:

- Absorbing boundary condition (the particle is always absorbed);
- Reflecting boundary condition (the particle is always reflected).

Our aim is to study the emptying process of a one dimensional system filled with a certain number of particles, following the same path we used in the previous Chapter where we considered absorbing boundary conditions. In order to develop analytical results for the Survival Probability and probability density function for the system under exam, we will focus on the Reaction-diffusion equation. Indeed, partially reflecting boundary conditions can be used in order to describe chemical reactions, which, together with diffusion, is a fundamental process in molecular biology [33]. During the following Chapter we will present a discussion about this kind of boundary conditions, developing analytical and numerical results in three peculiar conditions:

- Channel filled with a single Brownian particle;
- Channel filled with many Brownian point-like particles;
- Channel filled with many Brownian particles with volume excluded effects.

3.1 Diffusion Processes

In order to take into account processes characterized by partially reflecting boundary conditions, we will focus on the diffusion of particles in the one dimensional interval $[0, L]$, where L is the length of the computational domain, for example the channel considered in the previous Chapters. Considering that in our simulations we do not have a great number of particles, we chose not to describe the system in terms of density $n(x, t)$ of particles at point x at time t. Instead, we introduced the evolution equation for the probability distribution function $p_1(x, t|x_0, 1, L)$ for the single Brownian particle, which will have the identical form as equation (1.7) in Chapter 2:

$$\frac{\partial p_1(x, t|x_0, 1, L)}{\partial t} = D\frac{\partial^2 p_1(x, t|x_0, 1, L)}{\partial^2 x}, \tag{3.1}$$

where D is the Diffusion constant. The general fist order Partially Reflecting boundary condition at $x = a$ (also called *Robin* boundary condition [28]) is the following:

$$D\frac{\partial p_1(a, t|x_0, 1, L)}{\partial x} = Kp_1(a, t|x_0, 1, L) \tag{3.2}$$

where the non-negative constant K describes the reactivity of the boundary and may in general depend on time. A reflecting boundary condition corresponds to $K = 0$ while fully absorbing one corresponds to $K = \infty$. Indeed, to prove this second statement let's divide all members of equation (3.2) for K:

$$\frac{D}{K}\frac{\partial p_1(a, t|x_0, 1, L)}{\partial x} = p_1(a, t|x_0, 1, L) \tag{3.3}$$

where we consider

$$\frac{\partial p_1(a, t|x_0, 1, L)}{\partial x} \neq 0. \tag{3.4}$$

By considering the limit for $K \longrightarrow \infty$ we obtain

$$p_1(a, t|x_0, 1, L) = \lim_{K\longrightarrow\infty} \frac{D}{K}\frac{\partial p_1(a, t|x_0, 1, L)}{\partial x} = 0, \tag{3.5}$$

which corresponds to the absorbing boundary condition. As we previously stated, Partially Reflecting boundary conditions can be modeled using the reaction-diffusion equation [33]. For this purpose let's consider a particle diffusing in a one dimensional domain $[0, L]$ which is absorbed by a boundary at a certain position $x = a$. As we said, the probability distribution function for a single Brownian particle subjected to this kind of motion can be described by the reaction-diffusion equation:

$$\frac{\partial p}{\partial t} = D\frac{\partial^2 p}{\partial x^2} - \bar{K}p\delta(x - a) \text{ for } x \in [0, L], t \geq 0, \tag{3.6}$$

together with the no-flux conditions, where D is the diffusion coefficient and $\delta(x-a)$ is the Dirac delta function. The last term, $\bar{K}p\delta(x-a)$, is the standard description of the reaction kinetics, localized on the boundary. The constant $\bar{K}$, which can be experimentally measured, can be linked to the constant K of equation (3.2) related to the Partially Reflecting boundary conditions [30], indeed it has been demonstrated that $K = \bar{K}$. In this context, instead of solving equation (1.7) together with the Partially Reflecting boundary conditions (3.2) we can focus on the reaction-diffusion equations(3.6) in order to study the dynamics of our one dimensional diffusive system. Indeed, the constant K can be linked to the rate of absorpion and its presence emphasizes the imperfection of the reflection, or absorption, having certain probabilities for a particle hitting the boundary to be reflected or absorbed. Such situation leads to the case of partially absorbing conditions we were looking for.

Let's focusing on the Diffusion Processes of a single Brownian particle. Since problems characterized by total reflecting conditions are easier to treat than the one defined by partially reflecting ones, in the following paragraph we will derive the relationship between the Green's function $p_1(x,t|x_0,1,L)$ which satisfy the radiation boundary condition (i.e. partially reflecting), and the Green's function $G_1(x,t|x_0,1,L)$ which satisfy a reflecting boundary condition at a certain point $x=a$. Let's consider, more generally, the presence of a certain number of partial reflecting points in positions $x=a_j$ for $j=1,...n$. The evolution equation for the probability distribution function $p_1(x,t|r_0,1,L)$ can be written as:

$$\frac{\partial p_1(x,t|x_0,1,L)}{\partial t} = Lp_1(x,t|x_0,1,L) - \sum_j K_j\delta(x-a_j)p_1(x,t|x_0,1,L), \tag{3.7}$$

where

$$\hat{L} = D\frac{\partial^2}{\partial x^2}. \tag{3.8}$$

On the other hand, the evolution equation for $G_1(x,t|x_0,1,L)$ will be the simple Fokker Planck equation (1.7) which has been solved in the previous Chapter:

$$\frac{\partial G_1(x,t|x_0,1,L)}{\partial t} = \hat{L}G_1(x,t,|x_0,1,L), \tag{3.9}$$

where tho operator L has the same meaning as the one considered in (3.8).

The solution of equation (3.9) can be considered as a Green's function, allowing us to transform (3.7) into an integral equation in the form of Dyson's equation:

$$p_1(x,t|x,1,L) = G_1(x,t|x_0,1,L) - \sum_j K_j\int_0^t d\tau G_1(x,t-\tau|a_j,1,L)p(a_j,\tau|x_0,1,L). \tag{3.10}$$

The analytical derivation of the previous equation can be found in the Appendix 1.

In this way, $p_1(x,t|x_0,1,L)$ depends only on its value at the special points $x=a_1,...,a_n$. Let's notice also that that the term of the form $K\delta(r-a)$ represent a fully absorbing point at $\vec{a}$ in the limit $K\longrightarrow\infty$ and partially absorbing point for finite K, as imposed by Robin

boundary conditions (3.2). In order to solve equation (3.10) we set $x = a_1, a_2 ... a_n$ in turn which leads to the self-contained systems of equations:

$$p_1(a_i, t|x_0, 1, L) = G_1(a_i, t|x_0, 1, L) - \sum_j K_j \int d\tau G_1(a_i, t-\tau|a_j, 1, L) p_1(a_j, \tau|x_0, 1, L). \tag{3.11}$$

These, in turn, can be converted into a set of n linear equations in the Laplace transform

$$\begin{cases} \tilde{p_1}(a_i, s|x_0, 1, L) = \int_0^\infty e^{-st} p_1(a_i, t|x_0, 1, L) dt \\ \tilde{G_1}(a_i, s|x_0, 1, L) = \int_0^\infty e^{-st} G_1(a_i, t|x_0, 1, L) dt \end{cases} \tag{3.12}$$

which can be written as:

$$\tilde{p_1}(a_i, s|x_0, 1, L) + \sum_{j=1}^{n} K_j \tilde{G_1}(x_i, s|a_j) \tilde{p_1}(a_j, s|x_0, 1, L) = \tilde{G_1}(a_i, s|x_0, 1, L). \tag{3.13}$$

Finally, the solution of this set of equations can be substituted into the Laplace-transformed version of eq (3.10) obtaining:

$$\tilde{p_1}(x, s|x_0, 1, L) = \tilde{G_1}(x, s|x_0, 1, L) - \sum_{j=1}^{n} K_j \tilde{G_1}(x, s|a_j, 1, L) \tilde{p_1}(a_j, s|x_0, 1, L). \tag{3.14}$$

Defining, as we have done in the previous chapters, the Survival Probability function at a certain time t as in equation (2.6), the transform of $S(t|x_0, 1, L)$ is:

$$\tilde{S}(s; x_0, 1, L) = \frac{1}{s} \left\{ 1 - \sum_{j=1}^{n} K_j \tilde{p_1}(a_j, s|x_0, 1, L) \right\}. \tag{3.15}$$

From this theory we can also derive the previously used definition for the Mean First Passage Time. In fact, when reactions occurs sufficiently quickly so that one can define an average reaction time T, this parameter can be calculated directly from the Laplace transform

$$T(x_0, 1, L) = \int_0^\infty S(t|x_0, 1, L) dt = \tilde{S}(0, s|x_0, 1, L). \tag{3.16}$$

3.2 Single partially reflecting point

In the previous section, we defined analytical tools which can be used to treat the case of a general number of partial reflecting traps in positions $x = a_j$ for $j = 1, ..., n$. In this section we will apply the theory explained in the previous one, to the simplest case that allows examinations in detail. Such case is constituted by a system with a single partially absorbing point, say at $x = a$. This situation can be found in many physical systems, for example by simply considering a biological channel filled with particles which can be either absorbed or reflected at the end of it. The partial absorption can be modeled by the presence of a particular particle of smaller size respect to the other ones positioned at the end if it. Particles hitting such smaller molecule, can either be absorbed, i.e. going out of the channel, or reflected back with some different probabilities.

In this situation, equation (3.10) can be explicitly solved, in fact we have:

$$\tilde{p_1}(a, s|x_0, 1, L) = \tilde{G_1}(a, s|x_0, 1, L) - K\tilde{G_1}(a, s|a, 1, L)\tilde{p_1}(a, s|x_0, 1, L), \tag{3.17}$$

giving:

$$\tilde{p_1}(a, s|x_0, 1, L)(1 + K\tilde{G_1}(a, s|a, 1, L)) = \tilde{G_1}(a, s|x_0, 1, L) \tag{3.18}$$

and then

$$\tilde{p_1}(a, s|x_0, 1, L) = \frac{\tilde{G_1}(a, s|r_0, 1, L)}{(1 + K\tilde{G_1}(a, s|a, 1, L))}. \tag{3.19}$$

By inserting this expression into equation (3.10) we obtain:

$$\tilde{p_1}(x, s|x_0, 1, L) = \tilde{G_1}(x, s|x_0, 1, L) - \frac{K\tilde{G_1}(x, s|a, 1, L)\tilde{G_1}(a, s|x_0, 1, L)}{(1 + k\tilde{G_1}(a, s|a, 1, L))}. \tag{3.20}$$

The corresponding equation for the Survival Probability will be then

$$\tilde{S}(s; x_0, 1, L) = \frac{1}{s}\left[1 - \frac{K\tilde{G_1}(a, s|x_0, 1, L)}{(1 + K\tilde{G_1}(a, s|a, 1, L))}\right]. \tag{3.21}$$

If we use the free space Green's function for $\tilde{G_1}$, then equation (3.21) and (3.20) give the Green's function and Survival Probability in the presence of a delta function sink term of strength K at $x = a$. It also can be seen that if we use a Green's function for $\tilde{G_1}$ satisfying a purely reflecting boundary condition at $x = a$, then equation (3.20) yields the Green's function satisfying a partially reflecting boundary condition (radiation), as it will be demonstrated in Appendix A. This is a useful result, in fact it is simpler to solve problems subjected to reflecting boundary conditions rather than comparable equations with Partially reflecting one.

Since equation (3.21) has been written in a general form, it is necessary to derive the analytical form for $G_1(x,t|x_0,1,L)$, i.e. the Green's function satisfying reflecting boundary conditions. Indeed, in order to evaluate the survival probability of equation (3.21), we need the Laplace transform of $G_1(x,t|x_0,1,L)$. In order to find the expression for $G_1(x,t|x_0,1,L)$ we have to solve (1.7) imposing the reflecting boundary conditions at the two extremes of the channel in positions $x=0$ and $x=L$. Such conditions involve the flux $j(x,t)$, and we have to set:

$$j(x,t)=0 \text{ for } x=0 \text{ and } x=L, \tag{3.22}$$

where the flux has the following general form:

$$j(x,t)=\Big[D-\frac{\partial}{\partial \vec{r}}D\Big]G_1(x,t|x_0,1,L). \tag{3.23}$$

In our case, given the easier form of the Fokker Planck equation, the previous one reduces to:

$$j(x,t)=-D\frac{\partial}{\partial x}G_1(x,t|x_0,1,L). \tag{3.24}$$

By considering the general solution (2.18) obtained in section 2.2, the current will have the following form:

$$j(x,t)=D\frac{\partial}{\partial x}[e^{-D\lambda^2 t}(A_\lambda \sin(\lambda x)+B_\lambda \cos(\lambda x))]. \tag{3.25}$$

This condition must be imposed at $x=0$ and $x=L$ giving:

$$-De^{-D\lambda^2 t}[A_\lambda \lambda \cos(\lambda 0)-B_\lambda \lambda \sin(\lambda 0)]=0 \tag{3.26}$$

and hence $A_\lambda=0$.From

$$De^{-D\lambda^2 t}B_\lambda \lambda \sin(\lambda L)=0, \tag{3.27}$$

defining for simplicity $B'_\lambda=\lambda B_\lambda$ we obtain

$$\sin(\lambda L)=0 \longleftrightarrow \lambda L=n\pi \ \forall\ n\ \in \mathbb{Z}. \tag{3.28}$$

The final solution of the single particle diffusing within a channel of length L with reflecting boundaries conditions is then:

$$G_1(x,t|x_0,1,L)=\sum_n B'_n \cos\Big(\frac{n\pi}{L}\Big(x+\frac{L}{2}\Big)\Big)e^{-D(\frac{n\pi}{L})^2 t}. \tag{3.29}$$

From the initial condition

$$G_1(x, t \longrightarrow 0|x_0, 1, L) = \delta(x - x_0) \tag{3.30}$$

we will obtain:

$$\sum_n B_n \cos\Big(\frac{n\pi}{L}\Big(x + \frac{L}{2}\Big)\Big) = \delta(x - x_0). \tag{3.31}$$

By choosing the right orthonormal base we will have

$$\begin{aligned} B_n &= \frac{2}{L}\int_0^\infty \cos\Big(\frac{n\pi}{L}\Big(x + \frac{L}{2}\Big)\Big)\delta(x - x_0) = \\ &= \frac{2}{L}\cos\Big(\frac{n\pi}{L}\Big(x_0 + \frac{L}{2}\Big)\Big). \end{aligned} \tag{3.32}$$

Eventually, for the global probability distribution function for a single particle subjected to a partially reflecting point in $x = a$ we can write:

$$G_1(a|x_0, 1, L) = \frac{2}{L}\sum_n \cos\Big(\frac{n\pi}{L}\Big(a + \frac{L}{2}\Big)\Big)\cos\Big(\frac{n\pi}{L}\Big(x_0 + \frac{L}{2}\Big)\Big)e^{-D(\frac{n\pi}{L})^2 t}. \tag{3.33}$$

In order to write this equation in the general form obtained at the beginning of this section (equation (3.21)) we have to evaluate the Laplace Transform of the previous equation as follows

$$\begin{aligned} \hat{p_1}(x, t|x_0, 1, L) &= \hat{G_1}(a|x, 1, L) = \\ &= \frac{2}{L}\sum_n \cos\Big(\frac{n\pi}{L}\Big(a + \frac{L}{2}\Big)\Big)\cos\Big(\frac{n\pi}{L}\Big(x + \frac{L}{2}\Big)\Big)\int_0^\infty e^{-st}e^{-D(\frac{n\pi}{L})^2 t}dt = \\ &= \frac{2}{L}\sum_n \cos\Big(\frac{n\pi}{L}\Big(a + \frac{L}{2}\Big)\Big)\cos\Big(\frac{n\pi}{L}\Big(x + \frac{L}{2}\Big)\Big)\Big(s + D\Big(\frac{n\pi}{L}\Big)^2\Big)^{-1}. \end{aligned} \tag{3.34}$$

The last equation obtained has to be inserted in equation (3.21) in order to obtain the Laplace Transform for the Survival Probability. By anti-transforming we get the Survival Probability with the time dependence we were looking for.

3.3 Two Partially reflecting points

In this section we will extend the theoretical and numerical analysis previously developed to another similar system. Such system is now a channel of length L filled with one or many Brownian particles subjected to Partially Reflecting boundaries, which represent the partial traps of the thesis title.

Such condition of partial reflection at the extremes is developed introducing at the ends of the channel two other particle of smaller size, which, for simplicity, will not be subjected to Brownian motion. Such particles sizes are chosen in order to not completely close the channel, leaving the space necessary for the Brownian particle to pass and exit from it. In this way, we can say that we have introduced polydispersivity in our system, because of the different particles sizes. The two particles at the extremes of the channel can also be seen as obstacles or traps, reminding to the situation of crowded environment, and their sizes let the probability of exit from the channel be non zero but still different from the one characteristic of completely absorbing boundary conditions. As we have done before, our aim is to obtain the analytical and numerical form for the Survival Probability function of the system under exam. Later in this section we will present also the same analysis for the system of many non-interacting particles with partially reflecting boundaries conditions. For the first thing, let's apply the theory developed in section 4.1 to the case of two partially reflecting points, say in positions $x = a$ and $x = b$. We can explicitly solve (3.10), in fact, taking advantage of the Laplace transform as we have done before we have:

$$\tilde{p_1}(x, s|x_0, 1, L) = \tilde{G_1}(x, s|x_0, 1, L) - \sum_{j=a}^{b} K_j \tilde{G_1}(a_i, s|j, 1, L)\tilde{p_1}(j, s|x_0, 1, L). \tag{3.35}$$

In order to simplify the notation from now on we will simply indicate $\tilde{p_1}(x, s|x_0, 1, L)$ with $\tilde{p_1}(x, s|x_0)$ Then we will have to set in turn $a_i = a$ and $a_i = b$, obtaining the following system:

$$\begin{cases} \tilde{p_1}(a, s|x_0) = \tilde{G_1}(x, s|x_0) - K_a\tilde{G_1}(a, s|a)\tilde{p_1}(a, s|x_0) - K_b\tilde{G_1}(a, s|b)\tilde{p_1}(b, s|x_0) + \tilde{G_1}(a, s|x_0) \\ \\ \tilde{p_1}(b, s|x_0) = \tilde{G_1}(x, s|x_0) - K_a\tilde{G_1}(b, s|a)\hat{p_1}(a, s|x_0) - K_b\tilde{G_1}(b, s|b)\tilde{p_1}(b, s|x_0) + \tilde{G_1}(b, s|x_0). \end{cases} \tag{3.36}$$

Solving the previous system, we are able to calculate the form of $\tilde{p_1}(a, s|x_0)$ and $\tilde{p_1}(b, s|x_0)$ which have to be inserted in equation (3.35) in order to find the general form for $\tilde{p_1}(x, s|x_0, 1, L)$. The two function $\tilde{p_1}(a, s|x_0)$ and $\tilde{p_1}(b, s|x_0)$ have the following expression:

$$\tilde{p_1}(a, s|x_0) = \frac{\tilde{G_1}(a, s|x_0) - K_b\tilde{G_1}(a, s|b)\tilde{p_1}(b, s|x_0)}{1 + K_a\tilde{G}(a, s|a)} \tag{3.37}$$

and

$$\tilde{p_1}(b, s|x_0) = \frac{\tilde{G_1}(b, s|x_0)}{1 + K_b\tilde{G_1}(b, s|b)} - \frac{k_a\tilde{G_1}(b, s|a)}{1 + K_bG\tilde{} - 1(b, s|b)}\Big[\frac{\tilde{G_1}(a, s|x_0) - K_b\tilde{G_1}(a, s|b)\tilde{p_1}(b, s|x_0)}{1 + K_a\tilde{G_1}(a, s|a)}\Big]. \tag{3.38}$$

Inserting the last two equation in (3.35) we can derive an analytic but not simple form for the probability distribution function for the single Brownian particle in a channel of length L subjected to two partial absorbing traps $\tilde{p_1}(x, s|x_), 1, L)$.

In the following section we will present our numerical results. We simulated three different cases:

- Single Brownian particle in a channel with one partial trap;
- Many point-like particles in a channel with one partial trap;
- Many interacting particles with volume excluded effects in channel with one partial trap.

3.4 Numerical Simulation

3.4.1 Single particle

Similarly to what has been done in section 3.2, we simulated the emptying process of our system in order to numerically build the Survival Probability function related. The system under examination is a channel of length 30 (lj LAMMPS units), with one single Brownian particle. Firstly we would like to simulate the simplest case, i.e. the channel with a single partially reflecting point, i.e. partial trap, at one extreme of it ($x = -15$). From such point the particle, beginning its motion inside the channel, can either exit or be reflected and keep moving in the opposite direction towards the channel's center. In order to represent a partially reflecting point we simply add a smaller particle in a fixed and stationary position $x = -15$. Then, we set the channel radius to be of an appropriate size in order to make possible for the particle inside it to pass the smaller one at the extreme and exit from the channel. The two particle interact with each other with a Lennard Jones potential ($\sigma = 1$ lj LAMMPS units) and the channel radius is set to $r = 2.5$ lj LAMMPS units. In order to have just one partially reflecting point, we fixed a totally reflecting wall Lennard Jones potential at the other channel extreme, which keeps the particle inside our system (see Figure 3.1). The system which has been modeled using LAMMPS simulator can be easily understood looking at the Figure below, which represents the channel partially blocked with one particle

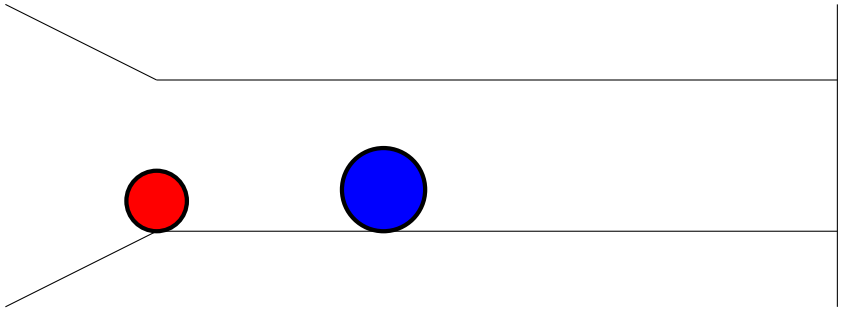

Figure 3.1: Channel system used in the numerical simulations performed with LAMMPS. The blue particle is a Brownian one, and our aim is to study its dynamics. The red particle instead is fixed at the extreme of the channel and its size has been chosen properly in order to partially block the red particle exit.

As we previously stated, our task is to build a numerical Survival Probability function for the system under exam. To do so, we used the emptying times of each simulation. Such values simply represent the instant when the single particle exits from the channel, passing over the partially blocking particle at the extreme $x = -15$. After having collected these data, we built a normalized histogram which represents the emptying probability $T(t|x_0, 1, L)$. The Survival Probability is then given by $S(t|x_0, 1, L) = 1 - T(t|x_0, 1, L)$. In the following Figure the Survival Probability for the single particles subjected to Partially Reflecting boundary condition (one partial trap in position $x = -15$) has been compared with the one for the single particle subjected to Absorbing Boundary condition. As we can see looking at Figure 3.2, absorbing boundary conditions speeds up the emptying process, indeed the particle subjected to its effects, at a given time has smaller probability to be still

inside the channel, i.e. it exits from the channel more rapidly on average than a particle subjected to Partially Reflecting Boundary condition.

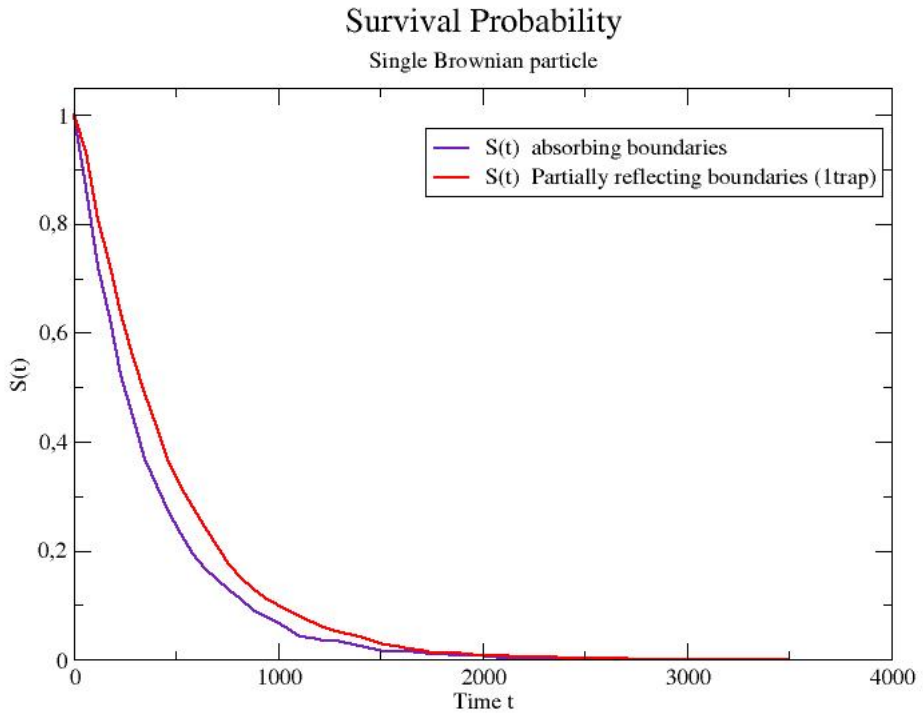

Figure 3.2: Time evolution of the two Survival Probability functions for the system described in Figure 3.1. In both cases, the right side ($x = 15$ (lj units)) is characterized by a wall potential, i.e. totally reflecting boundaries condition. The other extreme ($x = -15$ lj units) represents a partially reflecting boundary condition for the red line, and an absorbing one for the violet one. The total length of the channel is $L = 30$ (lj units) averaged over 1000 simulations.

In Section 3.2 we derived the analytical solution for the Survival Probability for a single Brownian particle within a channel of length L (3.21) which has been evaluated in the form of a Laplace transform. In order to look at the compatibility between analytical and numerical results, we compared the Laplace transforms of these two Survival Probabilities after having evaluated the Laplace transform of the numerical one. The coefficient K which appears in the analytical $\tilde{S}_1(s|x_0, 1, L)$ is linked to the reflection rate related to partially reflecting boundary conditions. Numerically such coefficient can be interpreted in many ways, for example it could be represented by the ratio between the channel space actually available for the exiting particles and the part of it which is occupied by the "obstacle" defining the partial reflecting boundary. In fact, with the partially reflecting boundary conditions, the channel ends are partly blocked by the presence of an obstacle. The space available is then the difference between the channel diameter and the blocking particle one. In the plot of the theoretical Laplace Transform of the Survival Probability, since the actual relation between the constant K of the partially reflecting boundary condition (3.2) and the probability of reflection is still a discussed topic [31], we simply considered K as a

fit parameter. In Figure 3.3 we plotted the Survival Probabilities transforms, verifying their compatibility.

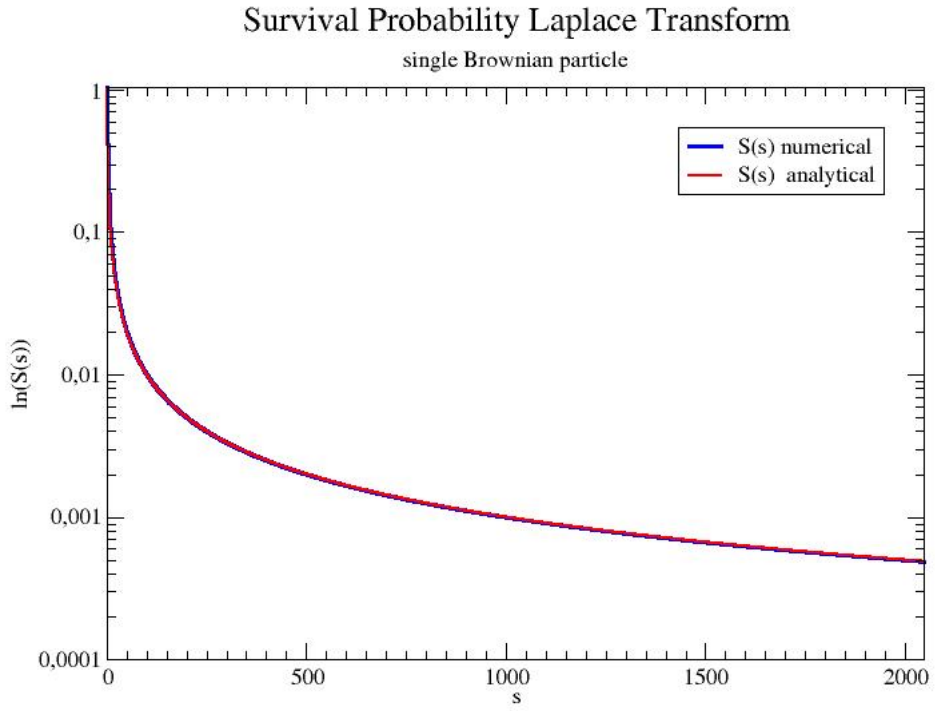

Figure 3.3: Comparison between analytical and numerical Survival Probability Laplace transforms. The analytical one has been plotted considering the coefficient K, which takes into account the reflection rate on partially reflecting boundary conditions, as a parameter.

3.4.2 Many point-like particles

By following the identical scheme used in the chapter 2 of this thesis, we will extend the analysis performed over the single particle subjected to partially reflecting boundaries to a system composed of many point-like particles. As we did in the case of absorbing boundaries conditions, volume excluded effects have been initially neglected. In this section we will consider a channel system filled with 6 particles in Single File without volume exclusion interactions among them. We chose a smaller channel length (L=30 lj units) in order to speed up the numerical simulations. The system, built using LAMMPS, is similar to the previous one: a channel with a cone at one extreme and a wall potential at the other one as in Figure 3.1. Such one dimensional system is now filled with many point-like particles, see Figure below:

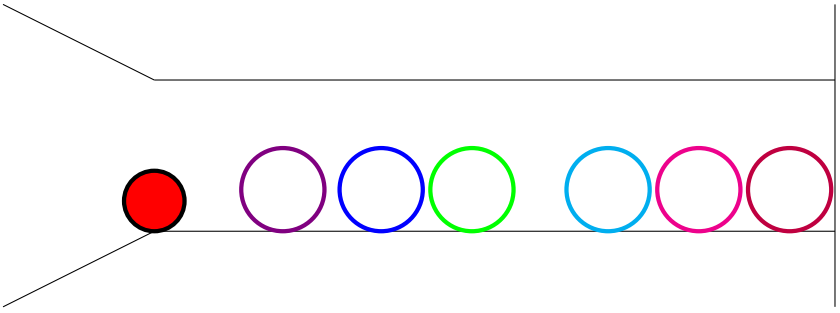

Figure 3.4: Channel system used in the numerical simulations performed with LAMMPS. The red particle is not subjected to the Brownian Dynamics, i.e. its position is fixed and it acts as partial trap. Its sizes has been chosen properly in order to partially block the other Brownian particles exit.

Following the same path used in all previous sections, we computed the Survival probability function $S(t|x_0, N, L)$, where N represents the number of particles in the system, i.e. the probability that a particle, started in a certain initial position x_0, will be still inside the channel at the time t. Again the Survival Probability has been evaluated through $S(t|x_0, N, L) = 1 - T(t|x_0, N, L)$. The following Figure 3.6 shows a comparison between three different functions $S(t|x_0, N, L)$ each of them related to a different case:

- many particles subjected to Partially Reflecting boundary conditions given by two partial traps at the ends of the channel;
- many particles subjected to Partially Reflecting boundary conditions given by a single partial trap at the right end of the channel;
- many particles subjected to Absorbing Boundary conditions.

As we can see from the Figure 3.6, similarly to the single particle case, the absorbing boundary leads to a more rapid channel emptying with respect to the Partially Reflecting one. Particles reaching the absorbing trap are forced to exit from the channel. On the other hand, particles reaching a partial trap, i.e. Partially Reflecting boundary, has a certain probability to be absorbed or reflected back, thus the emptying process is slower than the Absorbing case. The last comparison which can be seen from the Figure 3.6 is between one and two partial traps. In the second case we eliminated the wall potential substituting

it with another cone in order to represent a Partially Reflecting boundary as on the other extreme, see Figure 3.5

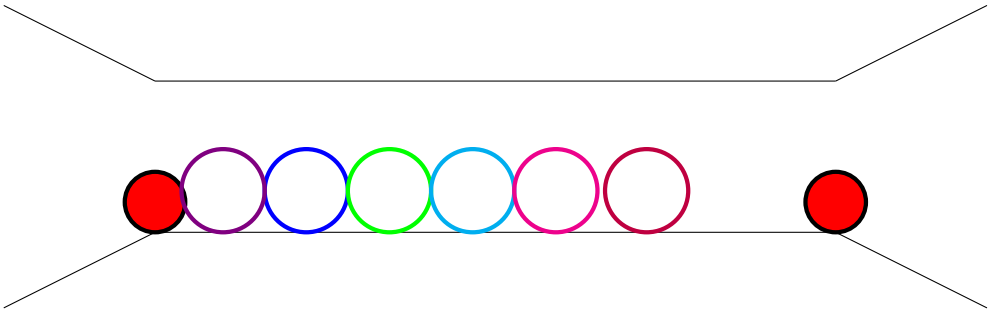

Figure 3.5: Channel system used in the numerical simulations performed with LAMMPS. The red particles are not subjected to the Brownian Dynamics, i.e. their positions are fixed and they act as partial traps. Their sizes have been chosen properly in order to partially block the other Brownian particles exit.

The comparison among the previoulsy cited Survival Probabilities can be seen from the following Figure 3.6

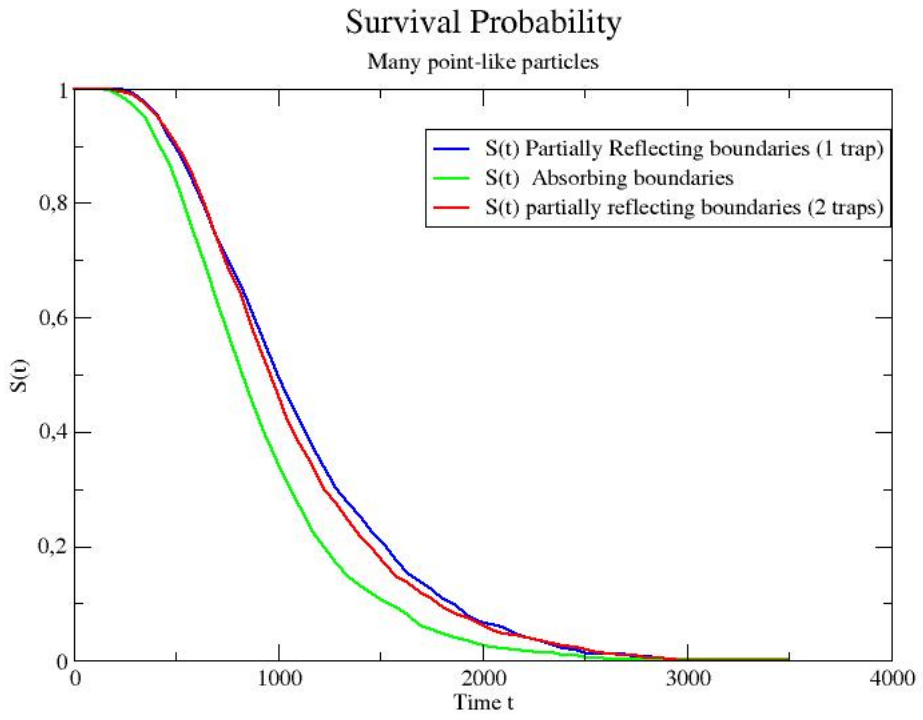

Figure 3.6: Time evolution of the Survival Probability function over time evolution of a channel system filled with 6 point-like particles described in Figure 3.5 and 3.4. The green line represents the $S(t|x_0, N, L)$ for the case of Absorbing Buondary conditions at one extreme. The blue line represent the analogue funcion for the Partially Reflecting boundary conditions of Figure 3.4, while the red one is the $S(t|X_0, N, L)$ for the system described in Figure 3.5. The total length of the channel is $L = 30$ (lj units) averaged over 1000 simulations.

In order to give an estimate of the errors related to this numerical Survival Probabilities function, we used the same approach as done in Chapter 2. We plotted the Survival Probabilities related to two different sets of 500 runs, then we evaluate the difference between the two functions obtained. Such value obviously fluctuates around zero and it has been used as the error associated to the function under examination for each time. As we can see from the Figure 3.7 the error bars progressively increase their sizes for higher time values. Such behavior relies on the worse statistic present for large times due to the low number of data in that part of the histogram.

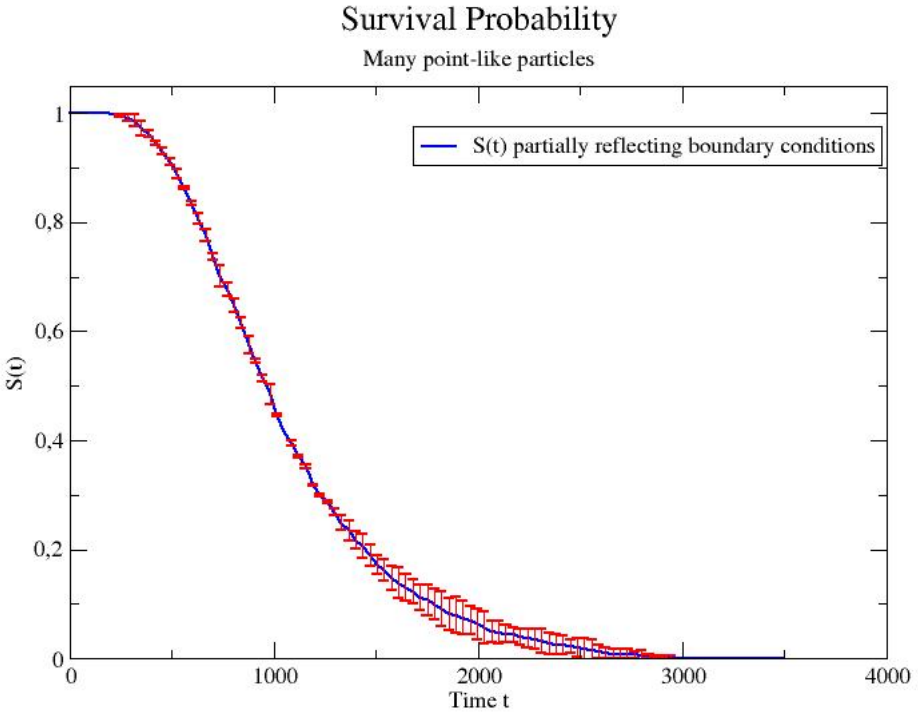

Figure 3.7: Time evolution of the Survival Probability function over time evolution of a channel system filled with 6 point-like particles described in Figure 3.4. The total length of the channel is $L = 30$ (lj units) averaged over 1000 simulations. We can notice that the size of error bars progressively increase for higher values of time.

3.4.3 Excluded Volume effects

The analytical derivation of the Survival Probability function cannot be easily obtained directly solving the Fokker Planck equation as it has been done for the non interacting case. From a numerical point of view, it is certainly possible to treat the more difficult case of a system composed by many particles characterized by excluded volume effects. The interaction taken into account can be modeled by considering a simple Lennard Jones potential among the considered Brownian particles.

In this section we focused just on the numerical treatment of the many interacting particles system, trying to find a form for the now well known Survival Probability function. In order to represent such $S(t|x_0, N, L)$ we followed the same approach used in all previous sections, simply adapting the numerical simulations to the case under exam. The system is similar to the one in Figure 3.4. As before we study the emptying process of the channel by collecting the exit times of each of the particles characterized this time by volume excluded effects.

These results are compared with the ones obtained considering a system of many interacting particles with volume excluded effects subjected to Absorbing buondary condition. Similarly to what we obtain in the previous section, where we considered point-like particles, the emptying process of a system subjected to Absorbing boundary condition is faster than the one related to a system subjected to Partially Reflected ones. The methods used in order to build the Survival Probability function are the same used in the previous sections. The cited comparison can be seen looking at the following Figure 3.8

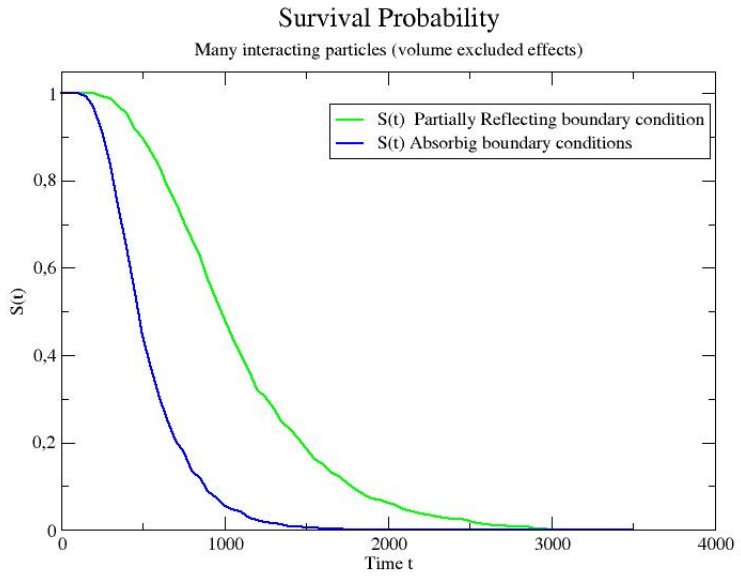

Figure 3.8: Time evolution of the Survival Probability function of a channel system filled with 6 particles subjected to a Lennard Jones potential among them which model the volume excluded effects. The system is the same used before, see Figure 3.4. The green line represents the $S(t|x_0, N, L)$ for the case of Absorbing Boundary conditions at one extreme. The blue line represent the analogue function for the Partially Reflecting boundary conditions

Conclusions

In this thesis we have investigated the properties of Single File systems of particles, devoting particular attention to absorbing and partially reflecting boundaries conditions. Recent progress on micro and nano scale fabrication and experimental techniques increased the interest and consideration devoted to Single File Diffusion, inspired by its scientific and technological relevance and by the emergence of pioneering experimental investigations [32]. Despite such interest and consequent increasing knowledge about such systems, many basic questions are still open, notably about the role of the boundary conditions.

Firstly, we have studied the dynamical properties of a Single File system of a point-like particle in the presence of two absorbing boundaries. Together with analytical calculations, such study has been performed trough numerical tools, simulating the system under examination with the molecular dynamic simulator LAMMPS. With respect to the analytical results, we have introduced the concept of emptying process and we have found the exact solution to this problem making use of the Reflection Principle Method, as explained in Chapter 1. The main focus has been given to the Survival Probability function $S(t|x_0, N, L)$, i.e. the probability of finding the considered particle, starting at an initial position x_0, at a certain time t still inside the channel. Such function has been evaluated analytically explicitly solving the Fokker Planck equation (2.32) for a single Brownian particle in a channel firstly considering absorbing boundaries conditions. Having found the analytical form for $S(t|x_0, N, L)$ we have looked for comparison with a numerical one, obtained trough simulations using LAMMPS. Computationally, we recreate a channel system with two cones at the ends of it interpreted as absorbing boundaries. The mayor entropy caused by increasing radius of the cones implies that once a particle exits from the channel, it will be really unlikely that it can come inside again. Having performed a consistent number of simulations, making an histogram of the exit times of all particles, we eventually obtained the numerical Survival Probability Function which, as it is reported in Chapter 2, has been successfully compared with the analytical one. The same dynamics analysis has been performed considering a channel system filled with many point-like particles. In this part of the thesis excluded volume effects have been neglected so that, remembering the random walk probability formula, we have been able to evaluate the analytical form for the Survival Probability function for the many particles system and eventually to compare it with the numerical one obtained again using LAMMPS.

Some attention has been given to the case of particles interacting with each others with a Lennard Jones potential. Such potential has been introduced in order to model the volume exclusion effects. This topic presents considerable analytical complications because of the lack of particles independence. Such difficulties made us able only to provide a numerical solution, again using LAMMPS simulator.

In the second, more original, part of this thesis we take into account another kind of boundary conditions: the partially reflecting ones, also called *radiation* boundary condi-

tions. Our focus has been given to the main differences which characterized this system with comparison with the one previously described. As we stated in Chapter 3, partially reflecting boundaries conditions represent a more realistic way to describe channel system characterized by Single File diffusion, being used to model a variety of common situations. Indeed, perfect absorption cannot be easily found in nature, as imperfect or partial traps are obviously more frequent. As we did for the case of absorbing conditions, we solved the Fokker Planck equation for the single Brownian particle this time subjected to a single partial trap in a certain fixed position. To do so, we relied on the Reaction-diffusion equation which takes into account the rate K between reflections and absorptions of particles. Making use of LAMMPS simulator we were able to numerically built the Survival Probability Function for the single Brownian particle in the presence of partially reflecting boundaries conditions, and to compare analytical and numerical results.

After having discussed the case of single Brownian particle, as we did in the previous chapter, we take into account a system composed of many point-like particle. Despite analytical difficulties, we performed numerous simulations in order to numerically build the Survival Probability function for the system composed by many interacting particles, subjected to a Lennard Jones potential among themselves. All numerical results have been then compared with the ones obtained in Chapter 2 related to the case of absorbing boundary conditions. As we would expect, Absorbing Boundary conditions cause a faster emptying process than the Partially Reflecting ones.

Concluding, we have done a systematic work to establish a coherent and comprehensive theoretical framework on the dynamical properties of Single File Systems, necessary also for comparing analytical results with numerical simulations. We also elucidated the role played by absorbing boundaries conditions as well as the main differences on particles dynamics caused by partially reflecting boundaries conditions. As future perspective, it would be highly desirable to take into account Active Single File studies, and compare such results with experimental data on bacteria and algae confined in microfluidic channel. In particular, cluster formation should be checked and the effect of an external bias should be investigated. It would be also of great interest the study of mixtures of passive and active particles, or even of bi- or poly-disperse active suspensions, in Single File conditions. These kind of mixtures in bulk have been used to investigate the microrheology of active suspensions, thus it would be useful to check the effects of confinement on such properties.

Appendix A

Relation between Green's function satisfying reflecting or partially reflecting boundary conditions

In this Appendix we will analyze in detail the relationship between the single particle Green's function $p_1(x,t|x_0,1,L)$ which satisfies the partially reflecting boundary conditions at $x=a$ and the Green's function $G_1(x,t|x_0,1,L)$ which satisfies a reflecting boundary condition at $x=a$. Our aim is now to demonstrate the relationship (3.10) which has been used in section 3.1 and let us describe the Green's function $p_1(x,t|x_0,0)$ in terms of $G_1(x,t|x_0,0)$ which has been evaluated in section 3.2 and have the form described by equation (3.34).

In this proof we will start from the Smoluchowsky equation, which describes the dynamics of Brownian particle subjected to an external force that can be expressed as the gradient of a potential $V(\vec{r})$. Such equation can be written in the following form:

$$\frac{\partial p_1(\vec{r},t|\vec{r_0},0)}{\partial t} = \bigtriangledown \cdot e^{-\beta V(\vec{r})} D(\vec{r}) \bigtriangledown [e^{\beta V(\vec{r})} p_1(\vec{r},t|\vec{r_0},0)] \tag{A.1}$$

Such Green's function is subjected to the radiation (partially reflecting) boundary condition:

$$D(r) e^{-\beta V(\vec{r})} \vec{n} \cdot \bigtriangledown [e^{\beta V(\vec{r})} p_1(\vec{r},t|\vec{r_0},0) = k p(\vec{r},t|\vec{r_0},0) \tag{A.2}$$

where $\vec{n}$ is a unit vector normal to the boundary at $\vec{r}=\vec{a}$ and directed towards the diffusion region. The Green's function $G_1(\vec{r},t|\vec{r_0},0$ also satisfies equation (A.1) but it is subjected to the reflecting boundary condition at $\vec{r}=\vec{a}$

$$\vec{n} \cdot \bigtriangledown [e^{\beta v(r)} G_1(\vec{r},t|\vec{r_0},0)] = 0 \tag{A.3}$$

In order to express $p_1(\vec{r},t|\vec{r_0},0)$ in terms of $G_1(\vec{r},t|\vec{r_0},0)$ we can start from the adjoint form of equation (A.1) for $G_1(\vec{r},t|\vec{r_0},0)$, derived from work [16]

$$-\frac{\partial}{\partial t} G_1(\vec{R},t|\vec{r_0},0) = e^{\beta V(r)} \bigtriangledown \cdot e^{-\beta V(r)} D(\vec{r}) \bigtriangledown G_1(\vec{R},T|\vec{r},t) \tag{A.4}$$

and the adjoint reflecting boundary conditions T $\vec{r} = \vec{a}$

$$\vec{n} \cdot \bigtriangledown G_1(\vec{R}, T|\vec{r}, t) = 0 \tag{A.5}$$

Multiplying equation (A.1) for $G_1(\vec{R}, T|\vec{r}, t)$ and (A.4) for $p_1(\vec{r}, t|\vec{r_0}, 0)$, we will obtain

$$\begin{aligned}
\frac{\partial}{\partial t}[G_1(\vec{R}, T|\vec{r}, t)p_1(\vec{r}, t|\vec{r_0}, 0)] &= G_1(\vec{R}, T|\vec{r}, t) \bigtriangledown \cdot e^{-\beta V(r)} D(\vec{r}) \bigtriangledown [e^{\beta V(r)} p_1(\vec{r}, t|\vec{r_0}, 0)] \\
&\quad - p_1(\vec{r}, t|\vec{r_0}, 0) e^{\beta V(r)} \bigtriangledown \cdot [e^{-\beta V(r)} D(\vec{r}) \bigtriangledown G_1(\vec{R}, T|\vec{r}, t)] = \\
&= \bigtriangledown \cdot \Big[G_1(\vec{R}, T|\vec{r}, t) e^{-\beta V(r)} D(\vec{r}) \bigtriangledown [e^{\beta V(r)} p_1(\vec{r}, t|\vec{r_0}, 0)] \\
&\quad - p_1(\vec{r}, t|\vec{r_0}, 0) D(\vec{r}) \bigtriangledown G_1(\vec{R}, T|\vec{r}, t) \Big]
\end{aligned} \tag{A.6}$$

Integrating the previous equation over r and t we simply obtain the following form

$$p_1(\vec{R}, T|\vec{r_0}, 0) = G_1(\vec{R}, T|\vec{r_0}, 0) - \int_0^T dt G_1(\vec{R}, T|\vec{a}, t) k p_1(\vec{a}, t|\vec{r_0}, 0) \tag{A.7}$$

As we can see, equation (A.7) is identical to equation (3.10), showing the relationships between the to Green's function satisfying the considered different boundary conditions.

Bibliography

[1] E. Frey and K. Kroy. Brownian motion: a paradigm of soft matter and biological physics. *Ann. Phys. (Leipzig)* 14:20-50,2005

[2] J.P. Bouchaud and A. Georges. Anomalous diffusion in disordered media: statistical mechanisms, models and physical applications. *Phys. Rep.*, 195:127-293,1990

[3] Anomalous diffusion models and their properties:non-stationarity, non-ergodicity and aging at the centenary of single particle tracking *Phys. Chem. Chem. Phys.* 2014, **16**, 24128

[4] A. Meller, L. Nivon and D. Branton. Voltage-driven DNA translocations through a nanopore. *Phys. Rev. Lett.* 86:3435,2001

[5] P.C. Bressloff and J.M. Newby. Stochastic model of intracellular transport. *Rev. Mod. Phys.*, 85:135-196,2013

[6] J. Caro and M. Noack. Zeolite membranes - recent developments and progress. *Microporous and Mesoporous Materials*, 115:215-233, 2008

[7] J. Kärger, M. Ruthven *Diffusion in Zeolites and in other Mcroporous Solids* Wiley, New York, 1992

[8] L. Peliti *Appunti di meccanica statistica* Bollati Boringhieri (2003)

[9] A. Corma. From microporous to mesoporous molecular sieve materials and their use in catalysis *Chem. Rev.* **97**:2373-2419, 1997

[10] E. Locatelli, E. Orlandini, F. Baldovin, M. Pierno, "Active Brownian Particles escaping a channel in Single File", Phys. Rev. E. **91** 022109 (2015).

[11] Delfau J.B., Coste C. and Saint-Jean M. 2011 *Phys. rev. E* **84** 011101

[12] Jepsen D.W.1925 *J. Math. Phys***6** 405

[13] C. Rödenbeck, J. Kärger and K.Hahn *Phys. Rev. E* 57:4382,1998

[14] G. Wilemski and M. Fixman, *J. Chem. Phys.* **58**:4009 (1973)

[15] A. Szabo, G. Lamm, G. H. Weiss, *Jour. of Stat. Phys, Vol 34, Nos 1/2* 1984

[16] A.Szabo, A.K Schulten, Z. Schulten, *J. Chem. Phys* **74**:4350 (1980)

[17] F. Baldovin, B. Marcone, E. Orlandini, A. Stella *Theory of topological disentanglement of linear polymers under stress*

[18] Q.H. Wei, /c. Bechinger and P. Leiderer. Single File Diffusion of colloids in one-dimensional channel. *Science* 287:625-627, 2000

[19] H. Risken *The Fokker-Planck Equation: Methods of Solutions and Applications.* Springer, 1996

[20] LAMMPS user Manual- Sandia National Laboratories Copyright (2003) Sandia Corporation.

[21] Mol. Phys. **81**, 475 1994

[22] J. Chem. Phys. **100**, 9140 1994

[23] *The Physics of Fluids in Hierarchical Porous Media: Angsotroms to Miles* (Kluvwer Academic, Bostonm 1997)

[24] S. Havlin and D. Ben-Avraham, Adv. Phys. **36**, 695 (1987)

[25] H. Scher and M. Lax, Phys. Rev B **7**,4491 (1973)

[26] A. R. Plastino and A. Plastino, Physica A, **222**, 347 (1995)

[27] F. Mota-Furtado and P. F. Omahony, Phys. Rev. E **75**, 041102 (2007)

[28] R. Erban and S. Jonatan Chapman *Reactive boundary conditions for stochastic simulations of reaction-diffusion processes* Phys. Biol. **4** (2007) 16-28

[29] *The Journal of Chemical Physics* **72**, 4350 (1980)

[30] Radek Erban and S. Jonathan Chapman, *Phys. Biol.* **4** (2007) 16-28

[31] A. Singer, Z. Schuss, A. Osipov and D. Holcman *Partially reflected diffusion* Siam. J. App. Math Vol **68**, No 3

[32] J. C. Crocker and D. G. Grier. Methods of digital video microscopy for colloidal studies. *J. Colloid Interface Sci.* 179:198, 1996

[33] Scott H.Northup and James T. Hynes. Coupling pf Translational and Reactive Dynamics for a Simple Lattice Model. *Journal of Statistical Physics* Vol. 18, N0 1, 1978